Chapter ??

PHOTONICS IN NATURE: FROM ORDER TO DISORDER

Villads Egede Johansen, Olimpia Domitilla Onelli, Lisa Maria Steiner, and Silvia Vignolini

University of Cambridge, Department of Chemistry, Lensfield Road, CB2 1EW, Cambridge, UK

Structural colours are widespread in nature, where a large variety of nanoscale structures give rise to a myriad of fascinating optical responses. These responses are often a combination of complex nanostructuring and hierarchical organisation. During the last few decades, the understanding of these photonic nanostructures and their response has improved greatly, mainly due to the development of imaging techniques and numerical tools to model light interaction (Vukusic & Stavenga, 2009; Vignolini et al., 2013).

So far, reviews about structural colours in nature have mainly focused on optical effects caused by interference of light from approximately regular periodic structures (Vukusic & Sambles, 2003; Kinoshita et al., 2008; Seago et al., 2009), even though biological organisms are often inherently structurally disordered (Kinoshita & Yoshioka, 2005). In fact, disorder can be a desired feature: specific optical appearances, such as angular independent colour response, silver or bright white diffuse appearances, rely on partially disordered or fully random structures, respectively (Prum & Torres, 2003b; Vukusic et al., 2007; Mäthger et al., 2009).

The investigation of these photonic nanostructures can help to address many questions in biological research, both in terms of their function and taxonomy (Bálint et al., 2012). It can, for example, contribute to investigations in evolutionary biology, or assessing the health of populations (Parker, 2000; Doucet & Meadows, 2009).

Moreover, structural colouration can have different functions, such as a cue to pollinators or for seed dispersal in some plants (Whitney et al., 2009; Vignolini et al., 2012). In some cases, it might be for camouflage, while in others it might be used for attracting mates (Seago et al., 2009; Wilts et al., 2014a). The repertoire is manifold, and many more studies are necessary to elucidate this interplay between structural colouration, function and behaviour.

Even though the field of structural colouration has progressed enormously over the last two decades, quantitatively assessing the role of order and disorder in photonic structures is still challenging. In Section 1, we introduce common approaches to detect periodicity and discuss light coherence. Then we consider ordered and quasi-ordered photonic structures, proceeding from 1D, via 2D to 3D in Section 2. We describe a few random natural photonic structures in Section 3. Finally, the complex interplay of order and disorder and colour mixing is described for hierarchical structures that are found at the surface of various organisms in Section 4.

1. THEORETICAL BACKGROUND

Light interference is the phenomenon at the basis of structural colouration in nature. When dielectric materials are organised periodically in space at a distance comparable to the wavelength of visible light, constructive and destructive interference occurs, providing intense metallic colourations with a strong angle-dependent behaviour (iridescence). By scrambling the periodic organisation, it is possible to drastically change the optical response, ranging from weak iridescence to matt colouration with no angular dependence to bright whiteness. It is therefore important to introduce methods to quantify periodicity in natural photonic structures, as we will return to these key concepts multiple times throughout the chapter.

Light coherence is also discussed, since the coherence properties of sunlight influence the overall appearance of ordered and disordered nanostructures.

1.1 The Fourier transform

Spatial periodicity can be quantified using the Fourier transform, which decomposes a function (most often a 1D profile or a 2D image) into its periodic components. The Fourier transform G of a function g in one dimension is given as

$$G(f) = \int_{-\infty}^{\infty} g(x) e^{-2\pi i x f} dx,$$

where f is the spatial frequency, x is the spatial dimension, and i is the imaginary unit (Lathi, 1998). For processing datasets (e.g. images) on a computer, a discretised version of the Fourier transform is required, for which the most common approach is the Fast Fourier Transform (FFT). The FFT is available in most math-oriented modern computer languages, such as Matlab, Python (numpy), and R. As an example, Fig. 1 shows the FFT analysis of the refractive index profile of an ideal artificial multilayer structure and an experimental dataset. In both cases, the periodicity can be extracted by reading out peak positions. The clear differences between peak values and backgrounds for the two examples indicate ordered structures. No peaks would be observable for completely disordered structures.

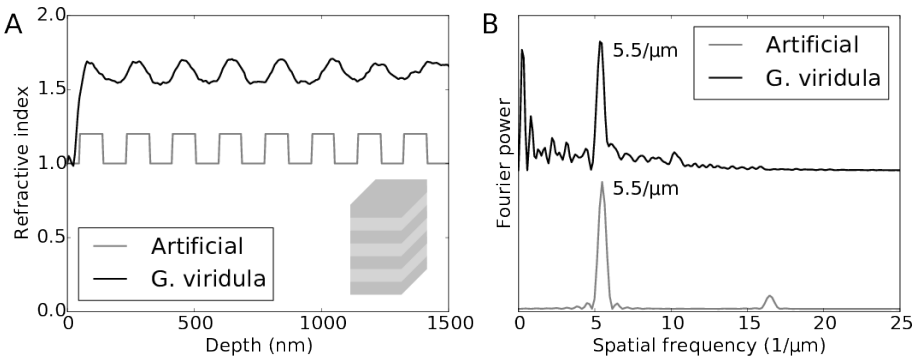

Figure 1. A: Refractive index profiles of an artificial ideal multilayer structure (see inset) and from the cuticle of a beetle (*Gastrophysa viridula*) extracted from Onelli et al. (2017). B: Zero-padded FFT of the two profiles normalised to the peak intensity. The inverse values of the peak spatial frequencies reveal a periodicity of roughly 180 nm. Periodicities that are a multiple of the main frequency (so-called harmonics) will normally also be present, thus explaining the extra peaks observed in both spectra. The distinction between peak and background signal is weaker for *G. viridula* than for the artificial example, but still very clear. In general, a larger difference between peak and background indicates a more ordered structure.

1.2 Structure factor and crystallography

Several other methods exist to detect periodicity. The mathematics behind the methods is generally similar to the Fourier transform in the sense that they also include integration or summation of complex exponentials.

In particular, the *structure factor* is useful to determine periodicity and correlations in two- and three-dimensional systems. For the structure factor, light is assumed incident from a specific direction on an ensemble of scattering elements that do not couple or shadow each other. In this configuration, the angularly resolved reflection or transmission of light is calculated based on information about the scattering elements and their positioning. The intensity of the structure factor I can be defined as

$$I(\boldsymbol{k_i}, \boldsymbol{k_o}) = \left| \sum_j f_j(\boldsymbol{k_i}, \boldsymbol{k_o}) e^{-i(\boldsymbol{k_i}-\boldsymbol{k_o})\cdot \boldsymbol{r_j}} \right|^2 ,$$

where $\boldsymbol{k_i}, \boldsymbol{k_o}$ are the vector incident and observation directions, respectively, scaled such that $|\boldsymbol{k_i}| = |\boldsymbol{k_o}| = 2\pi/\lambda$ where λ is the wavelength; $\boldsymbol{r_j}$ is the vector coordinate of the center of the j'th scatterer; i is the imaginary unit; and f_j describes the scattering intensity for the j'th scatterer.

If there is a periodic correlation of the distribution of scattering elements, this will show as strong reflection peaks at specific angles. A comparison between the structure factor for a periodic system and one with random perturbations is given in Fig. 2. A decrease in peak intensity is associated with a decrease in order, and the angular position can be calculated from the periodicity d through the grating equation (Johansen, 2014)

$$d \sin \theta_m = m\lambda,$$

where λ is the wavelength of incident light, θ_m is the m'th reflection angle, and m is an integer known as the grating order and is calculated as the number of peaks from the specular reflection. For the example in Fig. 2, where d=2.5λ, the peak locations for m=1, 2 are 23.6° and 53.1° respectively. The methodology can be applied in several ways for assessing disorder.

Small/Wide-angle X-ray scattering (SAXS and WAXS) is used to investigate order-disorder properties experimentally (Noh et al., 2010). In this technique, the sample is illuminated by X-rays with a wavelength in the 0.1 nm range and transmission at different angles is recorded. Similar to Fig. 2, the peaks in the angle-resolved transmission spectrum can be associated

with spatial correlation. The underlying theory is again very similar to that of the Fourier transform (Sellers et al., 2017).

Reflection from disordered surfaces can be predicted using the structure factor. More details on the theoretical background is given in Johansen (2014), and experimental validation and assessment of the quality of prediction is given in Johansen et al. (2015).

Structural analysis of scatterers can also be performed using the structure factor even if the scatterers couple and shadow each other, as long as the positions of the scatterers are known. In this case, the structure factor does not necessarily predict the optical response, but it works as a quantitative description of even advanced types of order/disorder relation such as hyperuniformity (Froufe-Pérez et al., 2016).

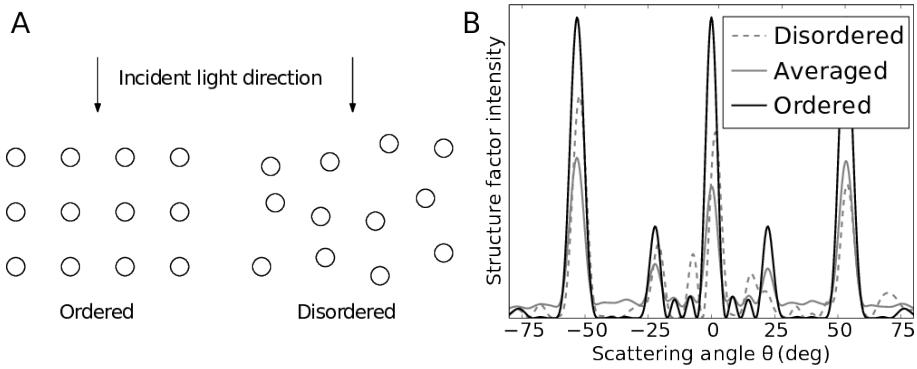

Figure 2. A: A strictly ordered system of 12 scatterers with $f_j = 1$ and a disordered system where the scatterers have been randomly displaced from their ordered lattice position. The lattice constant (separation) is 2.5λ. B: Intensity of the structure factor with respect to angle calculated for the systems in A. It is observed that for complete order, the response is confined to a few angles with very strong intensity. For the disordered realisation (dashed), the same peaks are present but with lower intensity, and a range of other peaks are seen. If such disordered samples are averaged over many random realisations taken from the same random distribution (unbroken), the effect is that the strong reflection angles are still present but less intense, with the remaining intensity almost evenly distributed in between.

1.3 Light coherence

Interference is caused by multiple reflections of light waves at interfaces between materials. The reflections can constructively or destructively interfere to promote an overall increase or decrease in reflection at specific

wavelengths. For this effect to occur, it is essential that reflected waves are coherent.

Mathematically, light waves are considered perfectly coherent if they are perfectly sinusoidal. In reality, this is not the case, as every light source is only coherent over a certain distance. Sunlight, for example, can be considered the sum of (randomly occurring) spontaneous emissions from the surface of the sun. This means that the wave profile from the sun deviates from a perfect sinusoidal shape and can therefore be described as partially coherent or incoherent. The degree of temporal coherence is most commonly described by coherence time τ_c or coherence length l_c, which are related parameters. These parameters indicate the length (in time or space) that the sinusoidal wave shape is correlated above a certain degree. The coherence area A_c similarly describes the area where correlation is observed for an illuminated surface (Wolf, 2007; Hecht, 2017). A small degree of correlation means that less intense interference effects can be observed for a given structure. For sunlight illumination, the coherence length is of the order of micrometers (Donges, 1998) and the coherence area of the order of $\sim 4 \cdot 10^3$ μm^2 (Wolf, 2007; Divitt & Novotny, 2015). The parameters vary depending on the environment (atmosphere, clouds, under water, etc.).

The degree of light coherence is rarely considered when analysing photonic structures. This is a valid approach if the photonic structures are small compared to the coherence parameters, since in this case light can be assumed coherent across the structures.

For larger structures, light cannot be considered coherent across the structure, but little is known about how this affects natural photonic structures and colouration. Bell et al. (2014) suggested that a locally ordered multilayer in a globally disordered arrangement makes the structural colour of the pyjama squid (*Sepioloidea lineolate*) unaffected by changes in light coherence properties, thus producing a consistent appearance in a changing underwater light environment. Dellieu et al. (2017) show how a structural colour system desaturates at short coherence lengths. The coherence area is also important for correctly predicting angle-resolved spectra from simulations, which would otherwise be dominated by strong, randomly located intensity fluctuations called speckle patterns. Saito and collaborators investigated this effect for a 2D natural photonic system, however the work has not been expanded since (Saito et al., 2011). It is therefore an area that deserves more attention as it may be an important factor for determining reflection and correlation properties in disordered natural photonic structures.

2. ORDERED AND QUASI-ORDERED PHOTONIC STRUCTURES

Most natural photonic structures are constituted by periodic arrangement of various materials on the nano- and micro-scale. We will start our discussion with one-dimensional structures and progress towards two- and three-dimensional ones.

2.1 One-dimensional photonic structures

The simplest example of a one-dimensional (1D) photonic structure is a thin film of dielectric material in air. When light impinges on the film, the rays reflected at the two surfaces interfere with each other. Whether this results in a constructive or destructive interference depends on the wavelength and incident angle of the light, the thickness of the film, and the refractive index of the dielectric medium (Kinoshita et al., 2008).

By stacking multiple layers with different refractive indices, it is possible to obtain multiple reflections when light impinges on the various interfaces. This can enhance the reflection in a specific spectral region (Fig. 3). These structures are generally referred to as "Bragg stacks" or "Bragg reflectors". In particular, it can be shown that the condition for constructive interference in a two-material repetitive structure for incident light of wavelength λ is

$$2(n_A d_A \cos\theta_A + n_B d_B \cos\theta_B) = m\lambda,$$

where n_A and n_B are the refractive indices of the two layers of thicknesses d_A and d_B, respectively; θ_A and θ_B represent the refraction angles for each of those and m is an integer (Kinoshita et al., 2008). Fig. 3, shows how the intensity of the reflected signal increases with the number of layers and how the response varies with the angle of incidence.

The most common multilayers in living organisms are made of pigments, usually melanin, arranged in layers alternating periodically (Land, 1972; Noyes et al., 2007).

Natural systems are generally regarded as perfectly periodic; however, it should be pointed out that these systems always have a certain degree of disorder. For example, in Fig. 1 the multilayer of the *G. viridula* beetle shows an imperfect layer periodicity. Furthermore, the refractive index changes gradually between the layers rather than in abrupt steps, as it is often modelled. This and other imperfections can lead to a significant mismatch between experimental data and theoretical calculations.

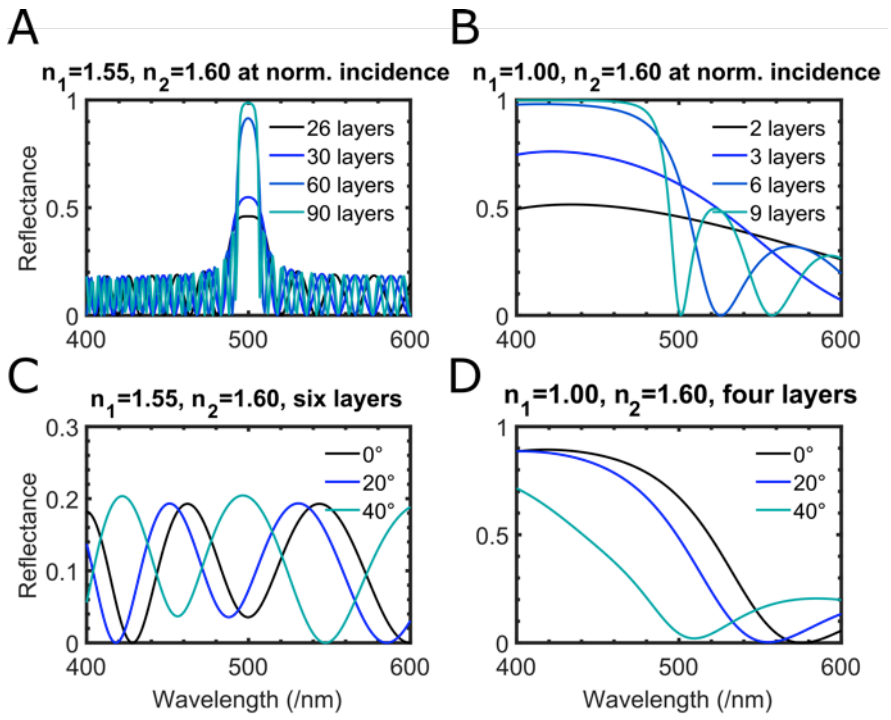

Figure 3. Modelling of periodic multilayers in air based on Kinoshita (2008) and carried out using open source code (Byrnes, 2016). A: Increasing the number of layers (indicated in the legend) increases the reflectance. B: The refractive index contrast between the layers is greater and therefore fewer layers are required to achieve a reflectance close to unity. The peak is now wider than in A. C and D illustrate the phenomenon of iridescence (i.e. the peak wavelength depends on the angle of incidence of the incoming light). The thickness of layer 1 is 81 nm; the thickness of layer 2 is 78 nm. The spectra are normalised with respect to an ideal mirror of unit reflectivity. The two TE and TM polarisations are calculated separately and averaged to simulate unpolarised light.

2.1.1 Periodic multilayers in nature

Periodic multilayers have been reported in a number of species (Hunt et al., 2007; Del Río et al., 2016). They are extremely frequent in beetles (Coleoptera), in which this effect has long been known (see reviews: Land, 1972; Parker, 1998). Researchers have recently investigated this phenomenon numerically (Noyes et al., 2007; Stavenga et al., 2011b) and also in relation to external inputs, such as for example an increase in water content (Mouchet et al., 2016). *In vivo* imaging of the development of the layered cuticle was conducted too (Onelli et al., 2017). The study showed how the deposition of the layers takes place before the polymerisation of the melanin.

Reports of keratin-based multilayer reflectors in avian feathers are also numerous (Prum, 2006; Nakamura et al., 2008; Stavenga et al., 2011a; Wilts, et al., 2014a). Interestingly, in these systems, the structural colouration is particularly conspicuous (Fig. 4) and serves mating purposes as opposed to most arthropod reflectors, which are considered to have camouflaging purposes (Seago et al., 2009). Bragg reflectors in the underwater world have been comprehensively reviewed (Denton, 1970). In the context of marine creatures, the refractive index contrast is provided by having anhydrous guanine crystals separated by cytoplasm, as shown in Fig. 4E-G (Gur et al., 2015). Guanine is highly birefringent, meaning that the refractive index of the crystals is different along the different axes. By arranging such crystals in different orientation, *Clupea harengus* (Atlantic herring) and *Sardina pilchardus* (European sardine) can reduce the polarising effect typical of multilayers to obtain a better camouflage whilst being able to reflect a large band of wavelengths (Jordan et al., 2012). Denton and Land also noted how the thickness of the layers was not perfectly periodic in the fish and cephalopods they investigated, which led to a lower peak intensity than in the ideal case (Denton & Land, 1971). However, this also means that the reflectors appear silver even for oblique incidence angles, which is the case for a fish illuminated by sunlight.

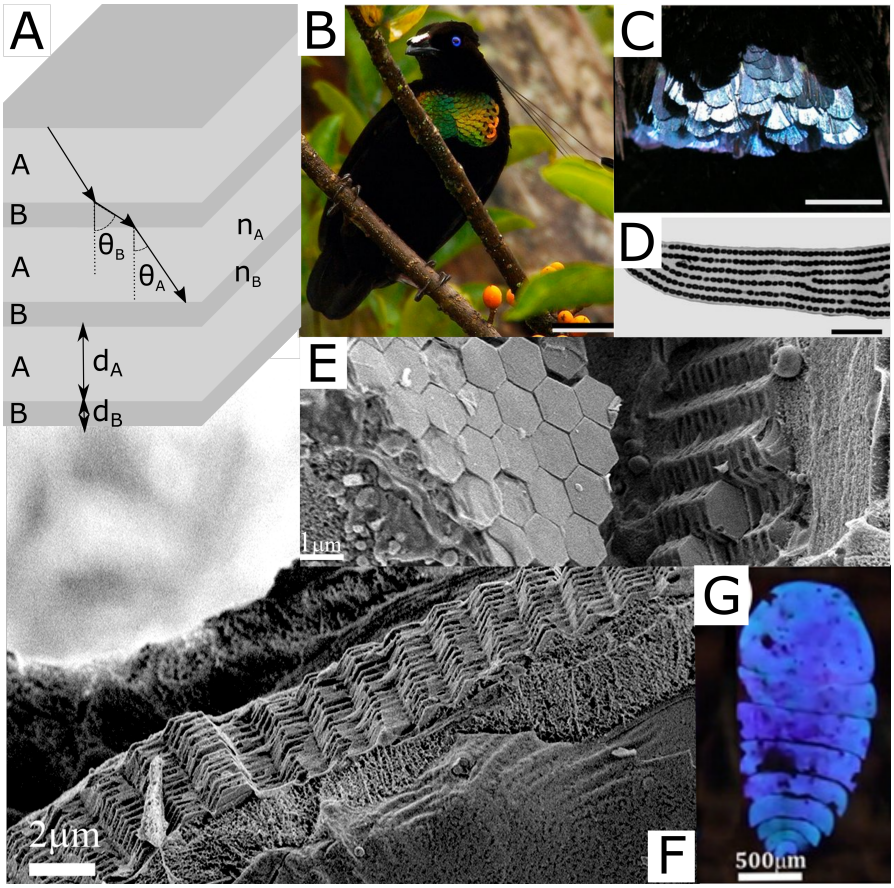

Figure 4. A: Scheme of a typical multilayer composed of two materials of refractive index n_A and n_B, respectively. B, C, D: The bird of paradise *P. lawesii* (scale bar: 5cm) and its mirror-like occipital feathers (scale bar: 1cm) imaged with TEM (scale bar: 2µm), respectively. Reproduced with permission from Wilts et al., (2014a). E, F, G: Guanine multilayer giving rise to the blue colouration in *Sapphirina metallina*. Adapted with permission from Gur et al. (2015), copyright (2015) American Chemical Society.

In the plant kingdom, many examples of multilayers can be found. Among land plants, the first multilayer example reported is the lycophyte *Selaginella willdenovii*. The optical response was first studied by Lee and Lowry and electron microscopy was later carried out by Hébant and Lee to confirm the existence of at least two layers atop the epidermal cells (Lowry & Lee, 1975; Hébant & Lee, 1984). Finally, the optical response was thoroughly analysed by Thomas et al. who proved that the iridescent colouration is indeed caused by a multilayer in the cuticle (Thomas et al., 2010). More examples of multilayers in plants leading to an iridescent appearance can be found,

including *Trichomanes elegans*, *Phyllagathis rotundifolia*, *Begonia pavonina*, *Elaeocarpus angustifolius* and *Delarbrea michiana* (Glover & Whitney, 2010).

More recently, Jacobs et al. found that thylakoid membranes in grana in iridoplasts in *Begonia pavonina* are arranged in multilayers, thus acting as photonic crystals, which enhance photosynthetic efficiency (Jacobs et al., 2016). This enhancement might be crucial in the extreme low-light conditions in the tropical forest understorey, and similar chloroplast structures have already been described in a phylogenetically diverse range of extreme shade dwelling plants.

In addition to those in the land plants, Bragg stacks are also found in some Rhodophyta (red algae). These algae display extracellular photonic nanostructures and have been recently analysed and reviewed (Chandler et al., 2017). For example, in the red alga *Chondrus crispus* the structural colouration is strongest at the tips of the frond, which constitute the youngest tissues (Chandler et al., 2015). The authors speculate that the loss of structural colour is due to the heterogeneity in the number and uniformity of the layers in the older parts of the alga. This is most probably due to the progressive deterioration and shedding of layers that are not regenerated, thus introducing disorder that suppresses the structural colouration.

2.1.2 Zig-zag, chirped, and fractal multilayers

Periodic structures typically reflect a narrow range of wavelengths. To achieve broadband reflectivity, it is necessary to vary the thickness (and/or the periodicity) of the layers in the stack so that a larger spectral range can be reflected efficiently. In the case of the beetles *Chrysina chrysagyrea* and *Anoplognathus parvulus*, the silvery colour originates from a chirped layering, where the thickness of each layer decreases in the direction of light propagation (Parker, 2005; Seago et al., 2009). A similar structure has been observed in the golden chrysalis of the butterfly *Euploea core* (Steinbrecht et al., 1985).

Another approach for obtaining a broadband silver reflection is the use of wavy multilayer reflectors as opposed to flat ones. This arrangement has been observed in the tissue surrounding the eyes of the squid *Loligo pealeii* (Mäthger et al., 2009).

In the blue-rayed limpet *Patella pellucida*, co-oriented layers of calcite give rise to an intense blue reflection that is remarkably angle-independent (Li et al., 2015). The strong optical response is the result of the introduction of complexity in the system: the multilayer is folded into a zig-zag pattern and the growth of the calcite is anisotropic, leading to the formation of

domains that have a different tilt with respect to the surrounding area. In addition, a completely disordered array of light-absorbing particles underneath the reflector attenuates the transmitted light, providing contrast to the reflected blue colour, even underwater, a strategy which is also known to occur in avian multilayers (Mason, 1923).

Completely disordered (or chaotic) reflectors have been reported (Parker, 2005), however more recent studies have found them to follow a fractal geometry (Bossard et al., 2016).

2.1.3 Helicoids

So far, we have mostly considered photonic stacks where the refractive index contrast between the layers is given by varying pigment content in alternating layers. Another strategy to produce bright colouration is to make helicoidal structures consisting of fibres arranged in birefringent layers (Middleton et al., 2017). In such structures, fibres lie parallel to each other in the plane, forming layers that are stacked on top of the previous one with a small rotation angle, thus forming a helicoidal architecture. This rotating arrangement gives rise to constructive interference when

$$\lambda = 2np,$$

where λ is the wavelength of the reflected light, n is the average refractive index of the material, and p is the pitch of the stack. The pitch p is defined as the distance between fibrils that have the same orientation, i.e. after the stack has completed a 180° rotation. The refractive index of living tissues typically lies between 1.0 and 2.0, so the response from the layers will be in the visible range only if the pitch is comparable to the wavelength of visible light, as predicted by the equation above.

In nature, various organisms show such structures: in plants, helicoids are made of cellulose fibres in their cell wall (Fig. 5A), whilst beetles (Coleoptera) display helicoids of chitin fibres in their cuticle. It is worth noting that helicoids can be right- or left-handed, thus only reflecting right- or left-handed circularly polarised light. Fig. 5B-C show such a helicoidal stack, the height of the pitch p, and how circularly polarised light is transmitted or reflected, depending on the handedness.

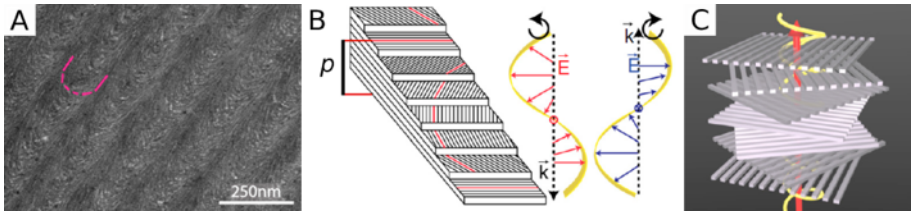

Figure 5. A: TEM of the helicoidal cellulose structure in the epicarp cell wall of *Pollia condensata*. The red lines correspond to the twisting direction of the cellulose fibres. B: (Left) Scheme showing a wedge of a left-handed helicoid with the arched pattern exposed on the oblique face, showing the height of pitch *p*. (Right) Beams of circularly polarised light. C: Scheme of a cellulose helicoid and a beam of transmitted circularly polarised light. A,C reproduced with permission from Vignolini et al. (2012). B adapted with permission from Wilts et al. (2014b).

In the plant kingdom, helicoidal arrangements are very common. However, in most cases the dimensions of the structure (the pitch *p*) are too large for interaction with visible light, producing no optical response.

Various plants from the ferns, monocots and dicots exhibit structural colouration caused by cellulose-based helicoidal structures. Among the ferns, the helicoidal cellulose arrangement of the fibres was first observed in the neotropical fern *Danaea nodosa*, via TEM (Graham et al., 1993). Interestingly, only juvenile leaves show the iridescent blue appearance. Adult leaves are green, and they exhibit considerably fewer and much less regular layers of helicoidal cellulose layers.

The same type of structure was observed in the Malaysian rainforest understorey plants *Lindsaea lucida* and *Diplazium tomentosum*, and characterised by spectroscopy and electron microscopy (Gould & Lee, 1996). The helicoidal arrangement of fibres is responsible for the blue, left-handed circularly polarised reflection.

Among the monocots, the fruit of the pantropical and warm-temperate perennial *Pollia condensata* (Fig. 6A-B), in contrast to the previous examples, shows both left-handed and right-handed circular polarised reflection. It is the only example of tissue in nature where helicoids of both handednesses are found (Vignolini et al., 2012). The epicarp contains three to four layers of cells with very thick cell walls that exhibit the helicoidal arrangement of cellulose fibres (Fig. 5A).

Another monocot reported in the literature is the tropical rainforest understorey sedge *Mapania caudata*, which only shows reflection of left-handed polarised light. It exhibits blue structural colour (see Fig. 6C-D) caused not only by the helicoidal cellulose arrangement in the adaxial epidermal cell wall, but also by the inclusion of silica granules into the cellulose layering (Strout et al., 2013).

In the class of dicots, the earliest report of helicoidal structures in plants is the work of Lee on the fruit of the rainforest tree *Elaeocarpus angustifolius* (D. W. Lee, 1991). However, these findings are not confirmed, since the reported electron micrographs showing the layering cannot resolve the cellulose fibres.

Finally, beautiful blue structural colour was also observed in the fruit of the dicot *Margaritaria nobilis* (Vignolini et al., 2016). Interestingly, the hydrated fruits exhibit metallic blue appearance but, upon drying, they turn pearlescent white. This effect is reversible and can be understood by changes in the ultrastructure that facilitates light absorption when hydrated.

In summary, there are still many plants with helicoidal cellulose fibre arrangements in their cell walls that have not yet been characterised. To our knowledge, researchers have not tried to assess the degree of disorder in these structures.

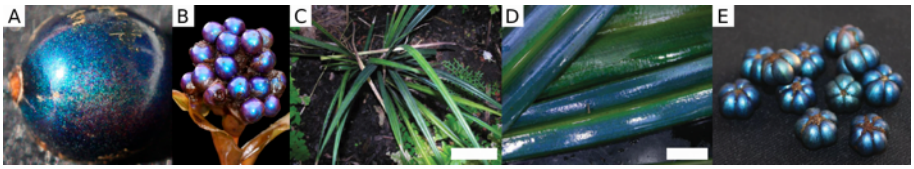

Figure 6. Pollia condensata A: Single dried fruit, B: Infructescence (cluster of fruits) from alcohol-preserved specimen; the diameter of each single fruit is about 5 mm. *Mapania caudata*: C: Young plants growing in shade, D: Edge of leaf to midrib. Scale bars 5 cm, 1 cm. *Margaritaria nobilis*: E: Fresh fruits. Diameter of each fruit is about 1 cm. A,B reproduced with permission from Vignolini et al. (2012). C,D reproduced with permission from Strout et al. (2013). E reproduced from Vignolini et al. (2016) licensed under CC-BY version 4.0.

Helicoidal chitin-based photonic structures have been observed in a number of beetle species (Coleoptera). Generally, such helicoids are responsible for the left-handed circularly polarised coloration of the beetles (Sharma et al., 2009). However, a few notable exceptions have been reported in which the cuticle can reflect both right- and left-handed light, such as *Chrisina resplendens* and *Chrisina boucardi (*Jewell et al., 2007) (note that both species used to belong to the genus *Plusiotis*, which has been placed

into synonymy under the older name, *Chrysina*, in 2001 (Arwin et al., 2012)). The physical explanation underpinning this phenomenon created disagreement for half a century (Michelson, 1911; Rayleigh, 1919; Neville & Caveney, 1969). Nowadays, the widely accepted interpretation is that the effect originates from the presence of a birefringent anisotropic layer between two left-handed helicoids, which acts as a half-wave phase retarder: left- handed light is reflected by the first helicoid, while right-handed light, transmitted through to the retarding layer, changes its polarisation from right to left and impinges on the second helicoid. At this point, the light (being left-handed polarised) is reflected and transmitted through the plate, which changes its polarisation back. Right-handed light is transmitted by the first helicoid, providing the additional right-handed reflected polarisation (Caveney, 1971; Hwang et al., 2005).

2.1.4 Diffraction gratings

Gratings are periodic surface undulations that give rise to strong angle-dependent light reflection when the feature sizes are comparable to the wavelength of light. The visual effect from a grating is generally experienced as an abrupt change of colour with respect to viewing angle. A well-known example is the compact disc (CD), see Fig. 7B, where data is stored between periodically spaced grooves that constitute a diffraction grating.

Gratings in nature were first reported in a scarab beetle in 1942, observed via electron microscopy (Anderson & Richards, 1942), and have found to be remarkably widespread in beetles from the order Coleoptera. Not much attention has been given to understanding the role of disorder in these structures, even though there seems to be a wide diversity of arrangements. Whether the biological significance of the gratings is the optical function or not (it might for example be to reduce friction) is still not understood (Seago et al., 2009).

As seen in Fig. 7, disordered grating-like structures have also been found in flower petals (Whitney et al., 2009). While the development of these structures is still not understood (Vignolini et al., 2013), their function seems important for plant-pollinator signalling (Whitney et al., 2009; Vignolini et al., 2015a; 2015b). The effect of the iridescence is hard to assess due to the subtle effect of the grating compared to pigmentation underneath, and many open questions remain (van der Kooi et al., 2014; 2015).

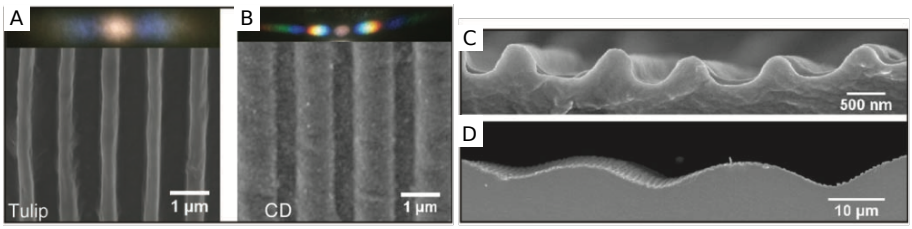

Figure 7. A: Top view of an epoxy cast of the tulip *T. kolpakowskiana*, showing striations resembling a line grating. Insert: the optical appearance of the flower in transmission under normal incident illumination. B: Top view of an epoxy cast of a disassembled CD. The insert shows how similar the reflection properties of a CD are in comparison to the surface of the flower. C, D: Cross-sectional view of the flower striations from A, showing the disordered arrangement of the individual scattering elements. The individual elements are arranged in a hierarchical manner on a structure with much larger undulations. Both hierarchical levels influence the appearance. Figure reprinted with permission from Whitney et al. (2009).

2.2 Two-dimensional photonic structures

In a two-dimensional (2D) photonic structure, the scattering elements vary in two dimensions while being invariant in the third one, see Fig. 8A. If the structural variations are periodic, such as in Fig. 8A, the system is referred to as a photonic crystal. Such photonic crystals give a specular reflection, but will also produce diffraction at a few discrete angles as exemplified in Fig. 2B, producing a glittering appearance that cannot be observed in one-dimensional multilayers (Fig. 9A).

The best known example of structural colour from a 2D structure is possibly the vivid appearance of peacock feathers (Zi et al., 2003), which originates from a regular packing of melanin rods and air channels in a keratin network that lies parallel to the surface of the barbule. Other examples of 2D regular and irregular packing with vastly different appearances are found in avian feathers (Prum et al., 1998), mammalian eyes and marine creatures (Starkey & Vukusic, 2013). More recently, 2D photonic structures have also been observed in bacterial colonies (Fig. 9) (Kientz et al., 2016).

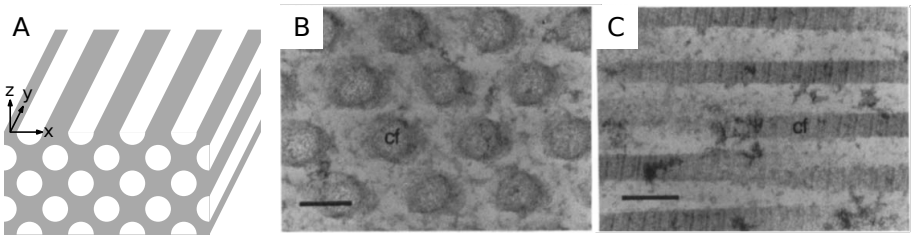

Figure 8. A: Scheme of a photonic crystal with a structure that is periodic in the *xz*-plane and invariant in the *y*-direction. B: TEM of a cross-section of an array of collagen fibrils found in the structure around the eyes of the velvet asity (*Philepitta castanea*). Scale bar: 100 nm. C: TEM of the longitudinal section of the collagen fibrils (with the distinct banding pattern being typical for collagen). Scale bar: 200 nm. Figure reproduced with permission from Prum et al. (1994).

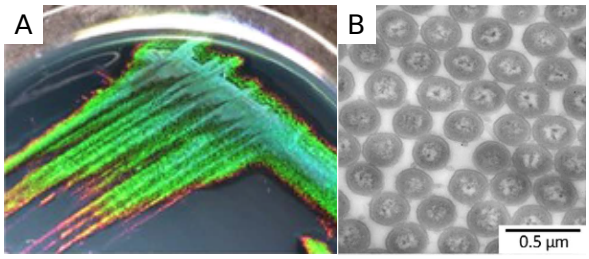

Figure 9. The colourful appearance of a bacteria colony of *Cellulophaga lytica* is caused by the rod-shaped bacteria packing in a roughly hexagonal arrangement as seen in B. The diffraction from this natural photonic crystal gives rise to the colourful appearance. The effect is yet to be observed in a natural environment, but readily reproduced in the lab (Kientz et al., 2016). Images from Kientz et al. (2016).

2.2.1 Modelling of photonic structures

Reflection maxima from periodic photonic structures (in two and three dimensions) can be computed by a so-called bandgap analysis using the open source tool MIT Photonic Bands (MPB) by the Massachusetts Institute of Technology (Johnson & Joannopoulos, 2001) or commercially available software by Comsol or Lumerical. Such investigations provide a band diagram that indicates which wavelengths can be expected to be fully reflected (Eliason & Shawkey, 2012). Even though this method does not provide the full spectral response, it provides a quick way to gain insight into a complex problem, and it constitutes a good starting point for understanding the optical response of a structure (Parker et al., 2001; Zi et al., 2003; Eliason & Shawkey, 2012). More details on photonic crystals can be found in the book by Joannopoulos et al. (2008), which is freely available online from the authors, and also in Yablonovitch (1993).

In order to fully describe the optical response from nanostructures (ordered or disordered), a full wave electromagnetic solver is needed. A

review of approaches deserves a chapter on its own, but it is worth mentioning that the Finite Difference Time Domain (FDTD) method is very popular within structural colour research, see for example Wilts et al. (2014a). The most popular tools are the open source software MIT Electromagnetic Equation Propagation (MEEP) (Oskooi et al., 2010) and the commercial software Lumerical FDTD.

2.2.2 Analysing order and disorder in 2D structures

The effect of disorder in 2D natural photonic structures was first investigated in the structure surrounding the eye of the velvet asity *Philepitta castanea* (Fig. 10C) (Prum et al., 1994). The structure consists of a 2D array of collagen fibres as seen in Fig. 8B-C. In this work, the authors conclude that even if the system lacks perfect ordering, it is still capable of supporting constructive and destructive interference, as also demonstrated in Benedek (1971), due to correlation in the structure factor, see Section 1.

Since 2D structures are invariant in the third direction, a cross-sectional image of the material is adequate to assess the degree of disorder of the entire structure. Fourier transformation (Section 1) of cross-sectional electron microscope images (e.g. Fig. 8B) is therefore a good method to reveal the fundamental level of periodicity in the structure. The approach was introduced (Prum et al., 1998) and further developed in the following decade by Prum and co-workers (Prum et al., 1999; Prum & Torres, 2003a; 2003b; 2013) and recently employed by other groups (Jordan et al., 2016).

The interplay between order and disorder in 2D photonic structures in birds is elucidated by Prum and Torres, who characterised an impressive number of species, showing a great diversity of optical effects (Fig. 10) (Prum & Torres, 2003b). The spectral responses were roughly estimated from the Fourier transform as well, whereas nowadays a better correlation can be obtained from the methods in Section 2.2.1. An interesting observation from the FFT spectra in Fig. 10G-H is the rotational symmetry. This implies that the periodicity of the system is the same in all directions perpendicular to the rods, which leads to decreased iridescence, and an appearance that will have the same reflection properties regardless of in-plane rotation. In contrast, the FFT in Fig. 10I shows a hexagonal pattern with clear spots, indicating direction dependence and a higher level of order, leading to a more angular dependent response. Such differences are hard to observe visually, since the overall optical appearance is affected by other factors such as pigmentation and feather orientation. The isolated photonic crystal response can, however, still be observed in small areas (Noh et al., 2010).

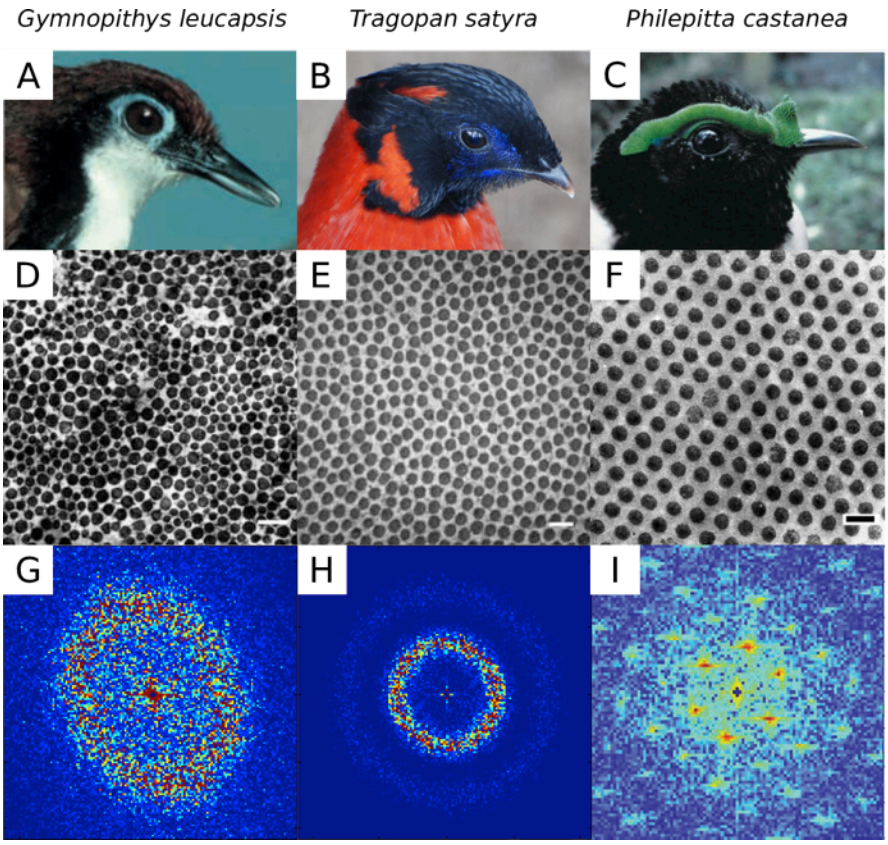

Figure 10. A, B, C: Photographs of three different avian species, whose feathers show photonic properties. D, E, F: Electron micrograph of the 2D photonic arrangements found in the feathers. Scale bar 200 nm. G, H, I: Fast Fourier Transforms of the electron microscopy images in D, E, F. The axis of the plots are all spanning -0.2 to 0.2 nm^{-1}. Images reproduced with permission from the author (Prum, 2003b) apart from B from Wikimedia Commons (2008).

As an alternative to Fourier analysis for the investigation of disorder, Delaunay triangulation was used to determine centre-to-centre distances between inclusions in the *Pherusa* worm (Trzeciak & Vukusic, 2009). This method provides additional statistical information about the relation between order and disorder in 2D natural photonic structures and can be more accessible for quantitative comparison than the Fourier transformed images. The approach is also used in Kientz et al. (2016) to assess the organisation of the bacteria colonies shown in Fig. 9.

By comparing the different examples presented in this section, it seems that for 2D photonic structures, disorder is not just an unavoidable feature in nature's photonic systems, but is used to control the optical response of the organisms.

2.2.3 Diatoms

A huge variety of photonic structures are found in the bio-mineralised silica cell wall of diatoms (Fig. 11) (Sumper & Brunner, 2006); here we classify them as 2D structures but, as we will see, some species can be considered three-dimensional. However, it is important to highlight that this categorisation is debatable as the photonic properties of diatoms might be a concomitant effect of their geometry and ultrastructures (Noyes et al., 2008).

In 2004 it was reported that the pores on the surface of the cell wall of *Coscinodiscus granii* act as a photonic crystal, selectively enhancing the transport of light towards the chloroplasts in the cell (Fuhrmann et al., 2004).

However, De Tommasi et al. (2010) later suggested that, for a similar species, *Coscinodiscus wailesii*, the nano-structured silica contributes to light diffraction. Numerical modelling showed how light is selectively confined within the edges of the pores according to its wavelength. The same species of diatoms was studied by Kieu and co-workers, who further investigated the role of the position of the pores. In fact, due to the imperfect periodicity of the pattern, the photonic structure in this system was defined as "quasi periodic" (Kieu et al., 2014).

Assessing disorder in diatoms' photonic structures can be challenging, however both Fourier analysis and X-ray diffraction experiments have been carried out (Almeida & Fujii, 1979; Yun et al., 1987). In the first study, the Fourier study was used to distinguish various species of diatoms for taxonomic purposes. The latter study was, instead, one of the first reports of X-ray diffraction measured in a microscopic, biological specimen.

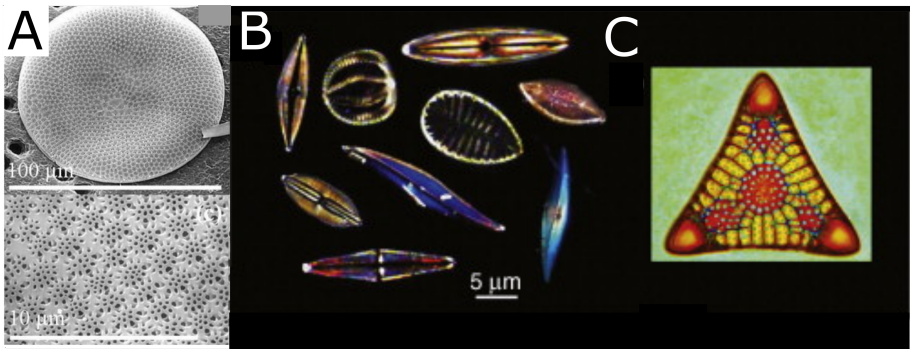

Figure 11. A: Scanning electron microscope images of the inner (top) and outer (bottom) valve of *C. wailesii*. B: micrographs of several pennate diatom species that show photonic properties. C: digitally enhanced Jamin-Lebedeff light microscopy image of the marine centric diatom fossil *Triceratium morlandii*. Cell width 120 mm. A adapted from De Tommasi et al., 2010, The Optical Society. B and C reprinted with permission from Elsevier, copyright (2009) (Gordon et al., 2009).

2.3 Three-dimensional photonic structures

Disentangling the roles that order and disorder play in three-dimensional (3D) architectures is extremely challenging because sophisticated 3D tomography methods, such as 3D X-ray and electron tomography, are necessary to investigate the architectures (Noh et al., 2010). Hence, three-dimensional structures are typically approximated by a unit cell, which is repeated periodically to form a highly ordered stack. Similar to 1D and 2D structures, when the periodicity of a 3D photonic crystal is comparable to the wavelength of visible light, only certain wavelengths will be reflected. Thus, 3D photonic structures can give rise to brilliant colours, which vary depending on the orientation of the photonic crystal with respect to the angle of incidence of light. The analysis tools to investigate these structures are analogous to the ones presented in Section 2.2.1.

2.3.1 Polycrystalline structures

In nature, such 3D structures are typically polycrystalline - meaning that the photonic structure is composed of a number of smaller crystallites (Seago et al., 2009). Each of the crystallites can be approximated by a perfectly repeating lattice, but the grains themselves can have different sizes and orientations. Hence, a polycrystalline structure has a high degree of

order within each domain but no correlation between the domains, causing colour desaturation and a more angle-independent response. This may here provide an evolutionary advantage due to a more consistent colour for signalling and camouflage (Michielsen & Stavenga, 2008).

In nature, diamond-like 3D photonic structures have been observed inside the iridescent scales of the weevils *Lamprocyphus augustus* (Galusha et al., 2008) and *Entimus imperialis* (Wilts et al., 2012b). In both cases, micron-size domains which are differently oriented guarantee an almost entirely angle-independent optical response.

In 1970 Alan Shoen, an engineer at NASA, discovered a 3D periodic structure, based on the mathematical concept of minimal surfaces, that he named *gyroid* (Schoen, 1970). This structure is composed of two distinct networks intertwined: one shows a six-fold geometry while the other is tetrahedral. Given the complexity and technically abstract nature of this crystal, the discovery of its occurrence in the cuticular structures of the lycaenid and papilionid butterflies is truly fascinating (Michielsen & Stavenga, 2008). Later, similar structures have been found responsible for the optical responses in various species such as *Callophrys rubi* (Michielsen et al., 2010; Schröder-Turk et al., 2011), *Cyanophrys remus*, *Parides sesostris* (Wilts et al., 2012a), and *Thecla opisena* (Wilts et al., 2017b). Just like in the case of the weevils, the crystalline structure is constituted of multiple domains with variable size and orientation as shown in Fig. 12. In fact, the absence of circularly polarised reflection (expected due to the inherent chirality of the gyroid network) in the wing of *C. rubi* and *Teinopalpus imperialis* has been attributed to disorder (Saba et al., 2014).

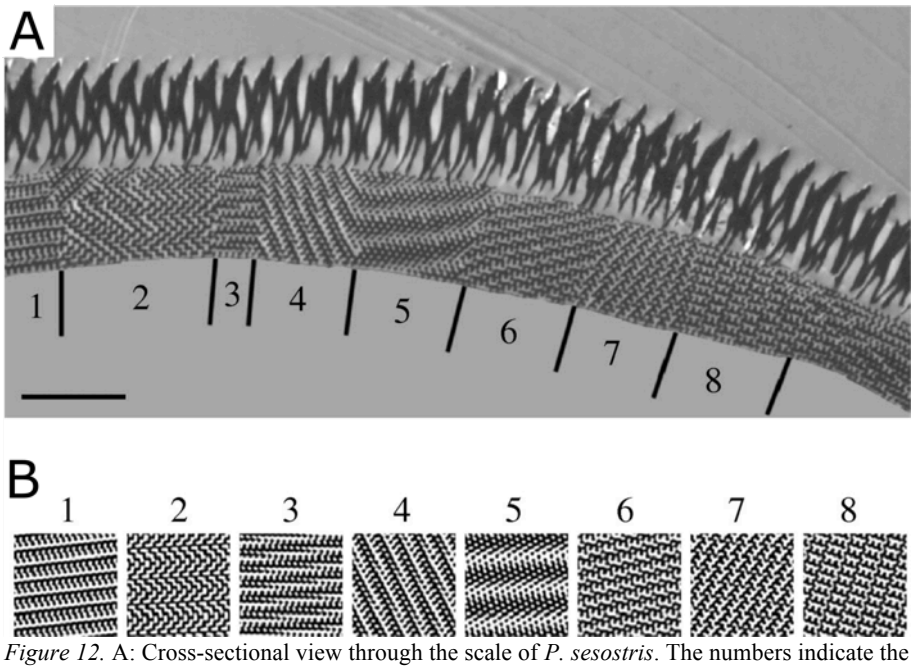

Figure 12. A: Cross-sectional view through the scale of *P. sesostris*. The numbers indicate the different domains in the cuticular crystal. The grain boundaries are indicated by vertical lines. Scale bar: 2.5μm. B: Projections of domains modelled computationally. Image reproduced from Michielsen & Stavenga (2008) licensed under CC-BY version 4.0.

2.3.2 Short-range ordered structures

Even in the absence of long-range ordering, structural colours can be generated if short-range periodicity is present. The colouration is much more diffuse in this case as reported and studied in detail in the beetle *Anoplophora graafi* (Dong et al., 2010). Another example of colour produced by short-range order is the complex keratin network in the blue feathers of the eastern bluebird *S. sialis* (Fig. 13A) (Shawkey et al., 2009). A 3D reconstruction of the tissue was obtained by electron tomography, and a subsequent Fourier transformation revealed a periodic arrangement of the material for the reconstructed model (Fig. 13B-C).

Another way of probing complex networks is by small-angle X-ray scattering (SAXS), see Section 1. The method has been used to analyse bird feather barbs (Noh et al., 2010) as well as the wing scales of the butterfly *C. gryneus* (Sellers et al., 2017).

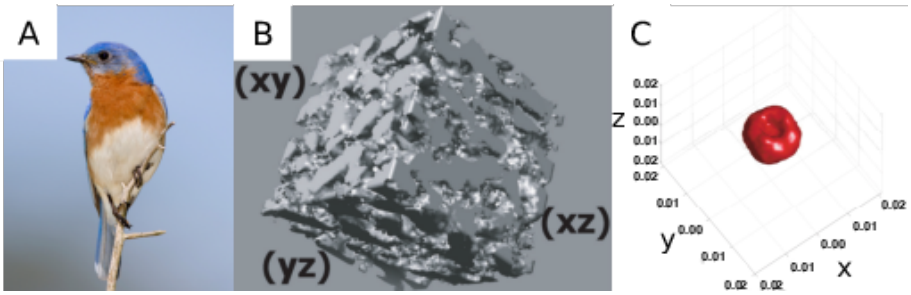

Figure 13. A: The eastern bluebird *S. sialis*. B: 3D reconstruction of the keratin structure in the feathers. C: 3D Fourier transform of the keratin structure. The doughnut shape reveals that the material is distributed periodically just like in Fig. 10G-H. This periodicity causes the blue colouration. Figure reproduced with permission from Shawkey et al. (2009) and Wikimedia Commons (2010).

3. RANDOM PHOTONIC STRUCTURES

Light propagating through a completely disordered structure will be scattered multiple times and exit the medium in random directions, thus giving a white, diffuse colouration (Wiersma, 2013). We can understand this phenomenon by considering each inhomogeneity in the medium's refractive index as a scattering centre: when light impinges upon one of these obstacles, it is scattered at a random angle and propagates until another collision occurs (Fig. 14A).

Natural random media can be extremely difficult to study and model, as the knowledge of their 3D morphology is challenging to obtain. However, the understanding of these systems is growing with availability of advanced tomography techniques, such as focused ion beam (FIB) milling and high resolution X-ray tomography that provide the required nm-resolution in three dimensions (Wilts et al., 2017a).

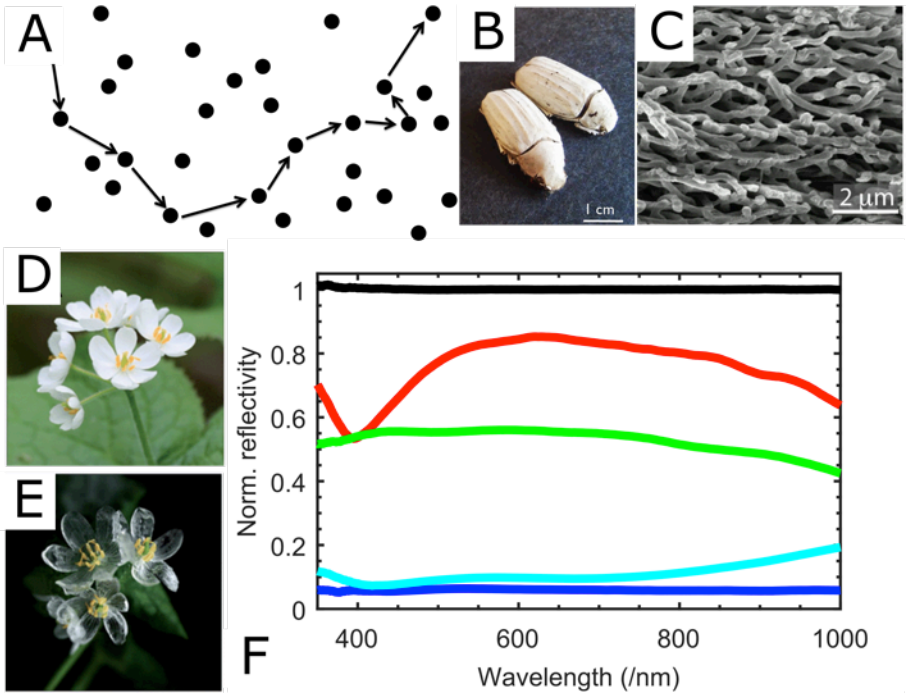

Figure 14. A: Light (represented by the arrow) is scattered multiple times by an inhomogeneous, complex medium (black dots). B: *Cyphochilus* beetles with their chitin network shown in C. Reproduced from Burresi et al. (2014) licensed under CC BY 4.0. D, E: Petals of *Diphylleia grayi* in sunlight and in the rain, respectively. Reproduced from Yong et al. (2015) with permission from The Royal Society of Chemistry. F: The reflectivity of various white materials compared to the white beetle *Cyphochilus* (red line). The green line corresponds to common filter paper (Whatman ®), the light blue to the hair of a polar bear (*U. maritimus*) and the dark blue to a transparent glass slide. The reflectivity was normalised with respect to a standard diffuser (black line). The numerical aperture of the microscope objective was 0.95.

The scattering strength of a standard diffusive material can be quantified by the average step length between the collisions. This quantity is known as the *scattering mean free path* and is used to compare the whiteness in different materials: a short mean free path implies that the scattering is very efficient, giving a whiter appearance. In fact, a long step length (i.e. the scatterers are inefficient) implies that light will be mostly unperturbed by the structure, leading to a transparent appearance of the material.

The scattering mean free path depends on three key parameters (Toninelli, 2007):

1. The size and shape of the scatterers. By comparing the dimensions of the scatterers with respect to the light wavelength, we can identify different scattering regimes (Akkermans & Montambaux, 2007). Intuitively, we see that if the obstacles are very small (i.e. much smaller than the wavelength of the incident light), light will not interact with them but will propagate as if the medium was homogeneous. Similarly, if the scattering centres are much larger than the wavelength, the medium will appear homogeneous, and light will propagate through it as in a bulk material.
2. The packing and density of the scatterers (or filling fraction). For efficient light scattering materials, the density of the scattering elements needs to be optimised. When the density of the scatterers is very low, the probability of having a scattering event decreases, making the material inefficient for scattering. However, if the density of the scatterers is too high, scattering from individual elements decreases as a consequence of the presence of others. This effect is known as optical crowding.
3. The refractive index ratio between the propagation medium and the scattering centres. If the difference between these two quantities is large, light will be scattered more efficiently. On the other hand, if the two refractive indices are similar, the medium will be effectively uniform.

3.1 Refractive index matching: *Diphylleia grayi*

The flower petals of the small herb *Diphylleia grayi* are white in dry weather. The numerous lacunae in between the cells on the petals are filled with air: the difference in refractive index between the two media causes light to be scattered and therefore produces a white colouration (Yong et al., 2015).

However, if it rains, the air gaps fill with water, whose refractive index is very similar to the one of cells. The petals become a uniform medium and light can propagate through them almost undeflected, giving a transparent appearance (Fig. 14D-E).

3.2 The whitest natural material: the *Cyphochilus* genus

Whiteness increases when there are a large number of scattering events. Thus, whiteness increases with thickness. In general, white materials are relatively thick, of the order of millimetres or larger. In the case of

Diphylleia grayi, the scattering events are probably not very efficient, however the tissue is thick enough to provide a white response. Similarly, polar bear hairs (*Ursus maritimus*) appear white not because the scattering events are particularly efficient (each hair is only slightly more reflective than glass, Fig. 14F) but because the overall fur is composed of numerous hairs that are arranged in layers. White paper is in comparison much more reflective than a single hair (Fig. 14F).

However, some organisms have extremely well optimised whiteness. The scales of the beetle genus *Cyphochilus* show a brilliant white colouration whilst only being 5-7μm thick, see image 14B-C. This makes them the whitest natural material known to date. The discovery was first reported in Vukusic et al. (2007), and it has been speculated that the white appearance helps the beetle camouflage amongst white fungi. Since then, many research groups have tried to explain how the *Cyphochilus* achieves such performance given that the biological material involved has a low refractive index and is therefore not well adapted for optimal whiteness. In fact, the scales are made up of long filaments of chitin, a long chain polysaccharide with a refractive index around 1.55-1.56.

By comparing *Cyphochilus* scales to other white beetles whose scattering efficiency is lower (*Lepidiota stigma* and *Calothyrza margaritifera*), it was observed that in all cases the filling fraction (i.e. the amount of chitin versus the amount of air) is optimised for scattering, but in *Cyphochilus* the scattering centres' spacing and diameters are particularly adapted to this function (Luke et al., 2010).

Time-resolved measurements confirmed that light is, indeed, scattered multiple times as it propagates through the scales (Burresi et al., 2014). The flux of photons through the scales was measured as a function of time elapsed from the illumination of the sample. This showed a significant time delay as compared to the time expected for light propagating ballistically (i.e. without being scattered). Later work demonstrated that the anisotropy of the chitin rod distribution was also important in the optical response (Cortese et al., 2015). In fact, the high filling fraction of the scales implies that some degree of angular correlation has to be introduced. In Fig. 14C it is possible to see such anisotropy as the chitin filaments are mostly distributed with a planar orientation.

Further measurements on *Cyphochilus insulanus* confirmed that the cuticle also shows a low degree of polarisation and gloss, which is a desirable characteristic in a camouflaging material (Åkerlind et al., 2015).

4. HIERARCHICAL STRUCTURES AT THE SURFACE

So far we have described structures on a scale comparable to the wavelength of light. However, the reflection properties can also depend on the hierarchical ordering of photonic elements on a larger scale and how these are distributed across a surface. In this section, two (among many) very different types of disorder on a meso- and macroscopic scale are described to exemplify the importance of hierarchical organisation for photonic properties and how disorder also plays a role here, namely diffractive surfaces and pixellated surfaces.

4.1 Diffractive surfaces on the *Morpho* butterfly wings

The interplay between order and disorder in the photonic structures presented in the previous sections can be used to obtain different optical effects ranging from strong iridescence to matt, diffuse colouration. However, even by varying the degree of order in these photonic materials, little freedom is provided to fully design the angular response of reflected light. This limitation can be overcome by hierarchically structuring the surface of the photonic material. The most well-known example is found in the scales of the *Morpho* butterfly.

4.1.1 Wing structure and appearance

The most studied structural colouration strategy in nature is probably the one used in the scales of several species of the *Morpho* butterfly, whose reflection properties were first quantified in 1999 (Vukusic et al., 1999). The colouration is mainly due to the distribution of long ridges of Christmas tree-like structures on the wing scales (Fig. 15). The nanostructuring of the ridges provides a colour reflection similar to a standard multilayer structure, see Section 2.1. Several other features, such as multiple layers of scales, scale tilt angles, and an absorbing background also influence the striking visual appearance of the butterfly (Ingram & Parker, 2008; Kinoshita et al., 2008; Giraldo et al., 2016). Vukusic et al. (1999) noticed that the reflection from the *Morpho* scales extended its blue colour roughly 100° along the longest direction and 15° along the shortest under normal illumination. This is illustrated by the elliptical shape in Fig. 16B. Such controlled reflectance properties are generally not easy to obtain.

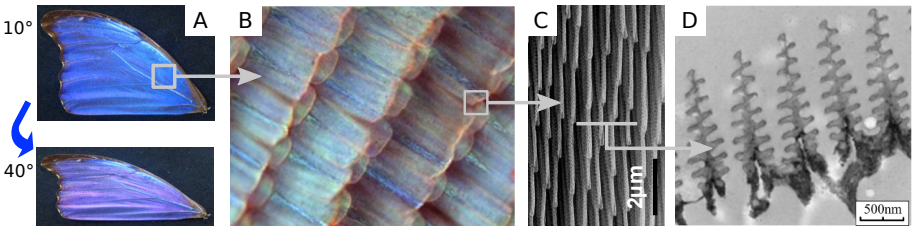

Figure 15. Hierarchical structuring on a *Morpho didius* wing. The ordering is typical for several *Morpho* species. A: Image of the wing from two different angles, showing iridescence caused by the structural colouration. B: Optical microscopy of the wing scales. The blue scales are covered by transparent scales. C: Top view of nanostructured ridges present on the blue scales. D: Cross-sectional view of the ridges in C, which are responsible for colour selectivity. A, C are reproduced with permission from the author (Saito et al., 2013). B, D reprinted with permission from Elsevier from Jiang et al. (2014).

Figure 16. Experiment to elucidate the reflection properties of the *Morpho* butterfly. A: The wing is mounted on the sample holder (light blue square) and illuminated through a hole in a screen. B: Photograph of screen in A, where the reflection from the butterfly wing is seen. The elliptical shape is caused by the anisotropic disorder properties of the nanostructures of the wing. A circular shape is much more common, both for pigmented and structurally coloured structures. The figure is reproduced with permission from the author (Saito et al., 2013).

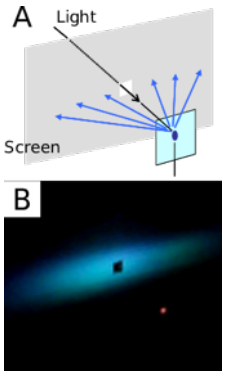

4.1.2 Hierarchical organisation

The physical mechanism behind the *Morpho* colouration was proposed by Kinoshita et al. to mainly rely on multilayer interference and the height difference between the individual ridges, which can be seen in Fig. 15C (Kinoshita et al., 2002). This interpretation inspired the fabrication of a surface mimicking the *Morpho*'s structural colouration only two years later (Saito et al., 2004). Since then, several contributions have uncovered more details in the understanding of the importance of disorder for the reflectance properties of the butterfly (Lee & Smith, 2009; Saito et al., 2011; Johansen, 2014).

In general, three disorder parameters seem crucial for reproducing the visual appearance of the *Morpho*: (i) the length distribution of the tree-like

ridges (Fig. 15C), which controls the angular width of the reflection cone in the compressed direction (cf. Fig. 16B); (ii) the width of each individual ridge, which determines the angular size of the reflection cone in the other direction; (iii) and the distribution of height displacements, which suppresses the diffraction grating effect normally obtained from periodic structures (like the ridges in a Compact Disc) in order to give a smooth angular reflection (Saito et al., 2006).

The diversity of structural colouration strategies found in butterflies suggests a large degree of tunability of the structures through evolution (Nijhout, 1985; Ghiradella, 1991; Wickham et al., 2006; Ingram & Parker, 2008), and there is also evidence that different types of disorder can provide similar results (Song et al., 2017). Given the impressive control of reflection properties that *Morpho* butterfly wings have, it is therefore likely that the scattering elements and disorder properties are highly optimised with respect to their optical response.

4.2 Pixellated surfaces

Pixellated surfaces can give rise to vivid metallic as well as inconspicuous colourations. We define pixellated colouration as the phenomenon that occurs when the macroscopic appearance of an organism is constituted by the individual reflections of many small units that are differently coloured so that their appearance can be resolved individually when magnified but not by the naked eye. Such small areas of different colour could be individual cells in plants, or single iridocytes, or the differently coloured areas could be e.g. caused by the strong curvature of wing scales of a butterfly. To our knowledge, pixellated surfaces have not been summarised and reviewed before, so we decided to classify them as in the list below. Each strategy will be discussed in more detail later in this section. Briefly, different ultrastructures have been found to provide a pixellated colouration in cases where:

- Individual units, like plant cells or iridocytes, reflect different wavelengths, e.g. *Pollia condensata*, *Margaritaria nobilis*, and *Tridacna maxima*.
- Individual units, such as iridocytes, reflect varying wavelengths within them, e.g. *Tridacna derasa*.
- The surface has areas or patches that reflect different colours, e.g. caused by different thicknesses in cuticular multilayers, e.g. *Cicindela oregona*, *Cicindela repanda*, and *Cicindela campestris*. This variation in layer thicknesses can also be linked to the structure of the surface, like in the elytra of *Chlorophila*

obscuripennis where the layer thickness is higher at ridges but lower in the basins.

- The surface is structured in a way that reflects different colours from different features, e.g. concavities made up of multilayers, with different colours reflected from the tops or the walls of the concavities, like *Papilio palinurus*, or butterfly scales with a strong curvature, like in *Chrysiridia rhipheus*. This effect is based on the angular dependency of reflection of multilayers.

Examples of pixellated appearance are the fruits of *Pollia condensata* and *Margaritaria nobilis* (Vignolini et al., 2012; 2016). In these fruits, each individual cell in the pericarp reflects a slightly different colour, by having a slightly different pitch in each cell, and the overall macroscopic appearance of the fruits is a metallic blue, see Section 2.1.3.

A similar example is the epithelium of certain clams (*Tridacna maxima*, *Tridacna derasa*), which has areas that show an intense white appearance, where individual iridocytes (cells that are Bragg-like reflectors) reflect different wavelengths (Ghoshal et al., 2016a; 2016b).

Whiteness can be caused either by the mixing of iridocytes of different colours, as in the case of *Tridacna maxima*, or by having different colours coming from just a single iridocyte, containing multiple Bragg stacks with different lamellar spacings, as in *Tridacna derasa*. Fig. 17A-B shows a juvenile *Tridacna maxima*, where the reflective epithelium of the mantle overlapping the shell is visible, and a close-up of a white investigated area. The microscope image 17E depicts an individual iridocyte, and a TEM of an individual iridocyte of the white area is shown in 17F, while a representative spectrum and the peak wavelength distribution are shown in Fig. 17G-H, respectively. A dissected *Tridacna derasa* and close-up of a white area are depicted in Fig. 17C-D.

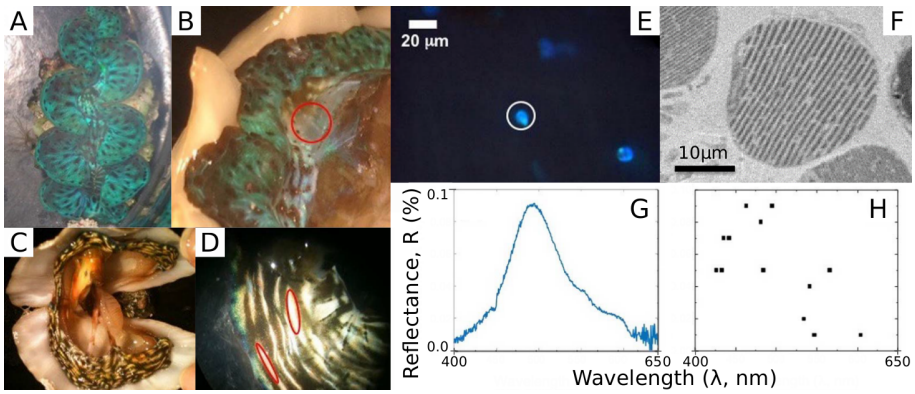

Figure 17. A: Juvenile *Tridacna maxima* (the length of the clam is 6 cm), B: and close-up. C: Photo and D: close-up of dissected *Tridacna derasa*. E-H *Tridacna maxima*: E: Microscope image of an individual iridocyte, F: TEM of iridocyte, G: Reflectance spectra and H: Colour distribution from individual iridocytes. A-E, G, H reproduced with permission from Ghoshal et al. (2016a). F courtesy of Daniel E. Morse.

The first example of colour mixing on pixellated surfaces was reported by Schultz and Bernard (1989) for tiger beetles. The dorsal wings of *Cicindela oregona* are covered by so-called alveoli, hexagonal pits of 13 µm across, consisting of cuticular multilayers. Fig. 18A shows a SEM of the elytral surface with clearly visible alveoli. Two different morphs of *Cicindela oregona* were investigated, a brown and a black one. The surface of the brown morph is structured by such alveoli and has patches of blue-green surrounded by a red field. The surface of the black morph has magenta patches surrounded by a dull green field. These different colours are obtained by different spacing of the cuticular multilayers. The different patches can be resolved by microscopy. The spectra at the microscopic scale were collected in an area of 30-40 µm diameter, comprising 5-8 alveoli of the same colour. However, at the macroscopic scale, the colours of the patches and the surrounding field mix and an overall brown or black appearance is observed. The spectral response at the macroscopic scale is measured on a 300 µm diameter area comprising around 530 alveoli and 7-8 colour patches. In this case, the reflectance is flat and unsaturated, giving the beetles a dull brown or black appearance, ideal for camouflage in their habitat.

The same macroscopic mixing effect is observed in the elytra of *Cicindela campestris*, see Fig. 18B (Berthier et al., 2007).

Finally, a similar mechanism is found in the elytra of *Cicindela repanda*, where blue-greenish *punctae*, surrounded by yellow circles in a red field

(Fig. 18C-F) can be distinguished at the microscopic scale, while at the macroscopic scale, the colours mix and give a dull brown reflectance (filled circles), comparable to wet sand (open circles), Fig. 18F, optimised for camouflage (Seago et al., 2009).

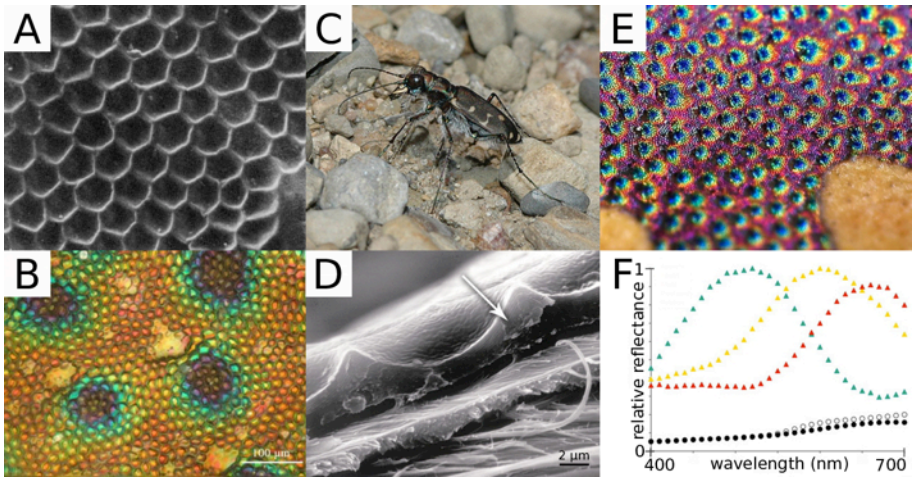

Figure 18. A: SEM of elytral surface of *Cicindela oregona*, each alveoli measures 13 µm across. B: Dorsal surface of elytra of *Cicindela campestris*. C-F: Photo, SEM, microscope image, and micro- and macro-scale spectra of *Cicindela repanda*, respectively. A reproduced with permission from Schultz and Bernard (1989). B reproduced with permission from Berthier et al. (2007). C-F adapted from Seago et al. (2009), courtesy of Thomas D. Schultz.

A similar effect is observed in the elytra of the beetle *Chlorophila obscuripennis* in Fig. 19A, which has a blue-green appearance. Here, the layer thicknesses of the chitin-melanoprotein multilayer are higher at the ridges than in the basins, so the bottom of the concavities reflects in the blue, while the sidewalls in the green (19D), as depicted in Fig. 19A-D. SEM (19B) and TEM (19C) images show the concavities built up of cuticular multilayers with thicker layers at the ridges and smaller layers in the basins (Liu et al., 2008).

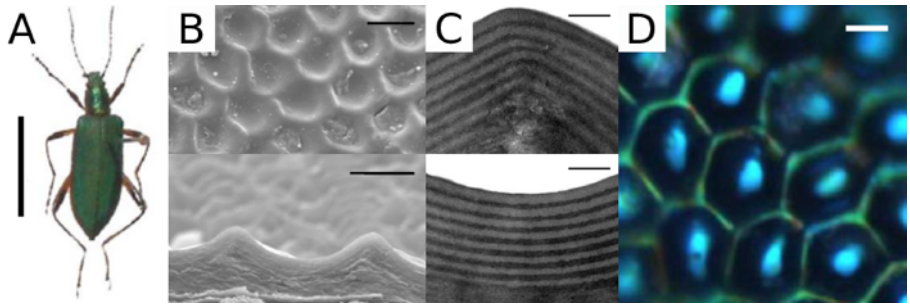

Figure 19: *Chlorophila obscuripennis*. A: Photo of *Chlorophila obscuripennis*, scale bar 1 cm. B: SEM of elytra: top view, and transverse cross-section, scale bars 10 µm, 5 µm. C: TEM cross-section of ridge and basin, scale bars 0.5 µm. Note the layer thicknesses are smaller in the basin region. D: Micrograph, scale bar 5 µm Reproduced with permission from Liu et al. (2008).

Another mechanism of pixellated colour is found in the butterfly *Papilio palinurus* (Fig. 20A) (Vukusic et al., 2000). In this case, the hierarchical surface structure consists of scales made up of multilayers. These multilayers are arranged in concavities of about 4-6µm in diameter and 0.5-3µm deep (Fig. 20B). The dimensions of the concavities are such that light reflected from the bottom of the structure shows a yellow reflection. In contrast, light impinging on the side walls of these concavities is reflected twice and yields an intense blue colouration, due to the different angle of incidence of the light with respect to the multilayer (Fig. 20C). Macroscopically, the contributions from the bottom and the side walls of these concavities cannot be resolved, and the butterfly wings look green.

A similar effect is found in *Chrysiridia rhipheus* (Fig. 20D) where the wing scales have a strong curvature (Fig. 20H) leading to light being directly reflected from the top of the curvature, and dual reflection for light impinging in between (see scheme in 20G). The distance between these two reflected bands is only around 200µm, so they cannot be resolved macroscopically (Yoshioka & Kinoshita, 2007; 2009).

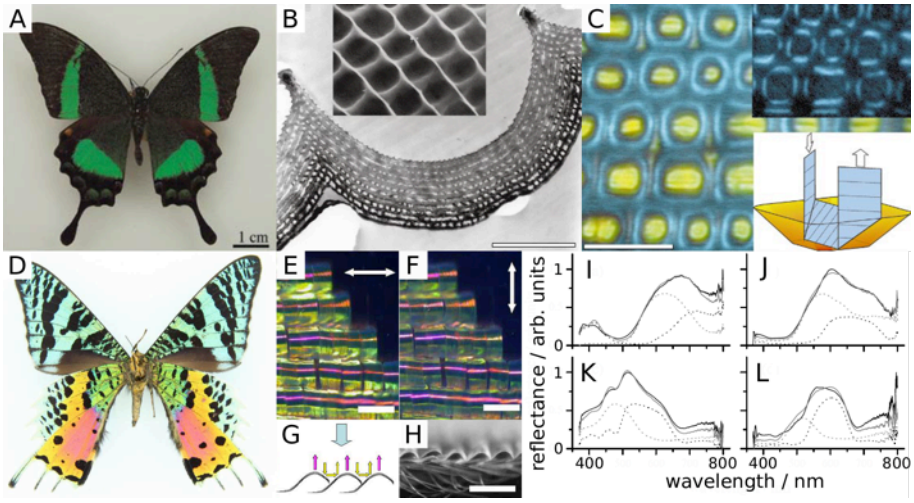

Figure 20. A-C: *Papilio palinurus*. A: Photo of *Papilio palinurus*. B: TEM of cross-section through concavity of an iridescent scale. Inset: SEM image of same surface. Scale bar, 1 µm (inset, 7 µm). C: Micrographs with unpolarised light, inset same area between crossed polarisers, and scheme, scale bar, 12 µm (inset, 6 µm). D-L: *Chrysiridia rhipheus*. D, E, F: Photo and microscope images (different polarisations) of *Chrysiridia rhipheus*, scale bar: 200 µm. G: Scheme of reflection from top and sides of curvature, and H: SEM cross-section, scale bar 300 µm. I-L: Reflectance spectra of purplish red, orange, pale blue, and green part of the wing, respectively. Individual (tops and bottoms of curvatures, black dashed and grey dashed lines) and additive spectra (taken by unfocusing the sample, black line, and summed from the individual spectra, grey line). A reproduced with permission from Sun et al. (2013). B, C reproduced with permission from Vukusic et al. (2000). D-H reproduced with permission from Yoshioka & Kinoshita (2007). I-L reproduced with permission from Yoshioka & Kinoshita (2009).

5. OUTLOOK

In summary, we conclude that disorder at different length scales adds functionalities to photonic structures in nature, providing control of colour and angular selectivity. In this chapter we reviewed examples of different types of disordered structures and their optical responses.

In contrast to perfectly periodic structures, where the knowledge of the unit cell is sufficient, the anatomical and theoretical description of disorder is very challenging because it requires the knowledge of the structures on a large area (larger than tens of microns) with nm-scale precision.

Investigation of disorder is a useful tool for understanding evolution and aiding taxonomic classification, with more results to come in the next few decades. At the same time, many of these principles will provide bio-inspiration for fabrication of new optical materials and further research will not only benefit biological understanding but also lead to new discoveries in other areas of science.

Acknowledgements This work was supported by a BBSRC David Phillips fellowship [BB/K014617/1], the European Research Council [ERC-2014-STG H2020 639088] and the European Commission [Marie Curie Fellowship LODIS, 701455]. The authors thank Rox Middleton for proofreading the manuscript.

REFERENCES

Akkermans, E., & Montambaux, G. (2007). *Mesoscopic Physics of Electrons and Photons* (pp. 36–70). Cambridge: Cambridge University Press.

Almeida, S. P., & Fujii, H. (1979). Fourier transform differences and averaged similarities in diatoms. *Applied Optics*, *18*(10), 1663-7. doi:10.1364/ao.18.001663

Anderson, T. F., & Richards, A. G. (1942). An Electron Microscope Study of Some Structural Colors of Insects. *Journal of Applied Physics*, *13*(12), 748. doi:10.1063/1.1714827

Arwin, H., Magnusson, R., Landin, J., & Järrendahl, K. (2012). Chirality-induced polarization effects in the cuticle of scarab beetles: 100 years after Michelson. *Philosophical Magazine*, *92*(12), 1583-99. doi:10.1080/14786435.2011.648228

Bálint, Z., Kertész, K., Piszter, G., Vértesy, Z., & Biró, L. P. (2012). The well-tuned blues: the role of structural colours as optical signals in the species recognition of a local butterfly fauna (Lepidoptera: Lycaenidae: Polyommatinae). *Journal of The Royal Society Interface*, *9*(73), 1745-56. doi:10.1098/rsif.2011.0854

Bell, G. R. R., Mäthger, L. M., Gao, M., Senft, S. L., Kuzirian, A. M., Kattawar, G. W., & Hanlon, R. T. (2014). Diffuse White Structural Coloration from Multilayer Reflectors in a Squid. *Advanced Materials*, *26*(25), 4352-6. doi:10.1002/adma.201400383

Benedek, G. B. (1971). Theory of Transparency of the Eye. *Applied Optics*, *10*(3), 459-73. doi:10.1364/ao.10.000459

Berthier, S., Boulenguez, J., & Bálint, Z. (2007). Multiscaled polarization effects in Suneve coronata (Lepidoptera) and other insects: application to anti-counterfeiting of banknotes. *Applied Physics A*, *86*(1), 123. doi:10.1007/s00339-006-3723-9

Bossard, J. A., Lin, L., & Werner, D. H. (2016). Evolving random fractal Cantor superlattices for the infrared using a genetic algorithm. *Journal of The Royal Society Interface*, *13*(114), 20150975. doi:10.1098/rsif.2015.0975

Burresi, M., Cortese, L., Pattelli, L., Kolle, M., Vukusic, P., Wiersma, D. S., et al. (2014). Bright-White Beetle Scales Optimise Multiple Scattering of Light. *Scientific Reports*, *4*, 6075. doi:10.1038/srep06075

Byrnes, S. J. (2016). Multilayer optical calculations. *arXiv e-prints, arXiv:1603.02720v2*.

Caveney, S. (1971). Cuticle Reflectivity and Optical Activity in Scarab Beetles: The Role of Uric Acid. *Proceedings of the Royal Society B: Biological Sciences*, *178*(1051), 205-25. doi:10.1098/rspb.1971.0062

Chandler, C. J., Wilts, B. D., Brodie, J., & Vignolini, S. (2017). Structural Color in Marine Algae. *Advanced Optical Materials*, *5*(5), 1600646. doi:10.1002/adom.201600646

Chandler, C. J., Wilts, B. D., Vignolini, S., Brodie, J., Steiner, U., Rudall, P. J., et al. (2015). Structural colour in Chondrus crispus. *Scientific Reports*, *5*, 11645. doi:10.1038/srep11645

Cortese, L., Pattelli, L., Utel, F., Vignolini, S., Burresi, M., & Wiersma, D. S. (2015). Light Transport: Anisotropic Light Transport in White Beetle Scales. *Advanced Optical Materials*, *3*(10), 1337-41. doi:10.1002/adom.201570061

De Tommasi, E., Rea, I., Mocella, V., Moretti, L., De Stefano, M., Rendina, I., & De Stefano, L. (2010). Multi-wavelength study of light transmitted through a single marine centric diatom. *Optics Express*, *18*(12), 12203-12. doi:10.1364/oe.18.012203

Del Río, L. F., Arwin, H., & Järrendahl, K. (2016). Polarizing properties and structure of the cuticle of scarab beetles from the Chrysina genus. *Physical Review E*, *94*(1), 012409. doi:10.1103/physreve.94.012409

Dellieu, L., Cael, G., Louette, M., Herman, A., Deparis, O., & Sarrazin, M. (2017). Light coherence time modifies color perception of living beings. *Materials Today: Proceedings*, *4*(4), 4952-8. doi:10.1016/j.matpr.2017.04.101

Denton, E. J. (1970). Review Lecture: On the Organization of Reflecting Surfaces in Some Marine Animals. *Philosophical Transactions of the Royal Society B: Biological Sciences*, *258*(824), 285-313. doi:10.1098/rstb.1970.0037

Denton, E. J., & Land, M. F. (1971). Mechanism of Reflexion in Silvery Layers of Fish and Cephalopods. *Proceedings of the Royal Society B: Biological Sciences*, *178*(1050), 43-61. doi:10.1098/rspb.1971.0051

Divitt, S., & Novotny, L. (2015). Spatial coherence of sunlight and its implications for light management in photovoltaics. *Optica*, *2*(2), 95-103. doi:10.1364/optica.2.000095

Dong, B. Q., Liu, X. H., Zhan, T. R., Jiang, L. P., Yin, H. W, Liu, F., et al. (2010). Structural coloration and photonic pseudogap in natural random close-packing photonic structures. *Optics Express*, *18*(14), 14430-8. doi:10.1364/oe.18.014430

Donges, A. (1998). The coherence length of black-body radiation. *European Journal of Physics*, *19*(3), 245-9. doi:10.1088/0143-0807/19/3/006

Doucet, S. M., & Meadows, M. G. (2009). Iridescence: a functional perspective. *Journal of The Royal Society Interface*, *6*(Suppl 2), S115-32. doi:10.1098/rsif.2008.0395.focus

Eliason, C. M., & Shawkey, M. D. (2012). A photonic heterostructure produces diverse iridescent colours in duck wing patches. *Journal of The Royal Society Interface*, *9*(74), 2279-89. doi:10.1098/rsif.2012.0118

Froufe-Pérez, L. S., Engel, M., Damasceno, P. F., Muller, N., Haberko, J., Glotzer, S. C., & Scheffold, F. (2016). Role of short-range order and hyperuniformity in the formation of band gaps in disordered photonic materials. *Physical review letters*, *117*(5), 053902. doi: 10.1103/PhysRevLett.117.053902

Fuhrmann, T., Landwehr, S., Rharbi-Kucki, El, M., & Sumper, M. (2004). Diatoms as living photonic crystals. *Applied Physics B*, *78*(3-4), 257-60. doi:10.1007/s00340-004-1419-4

Galusha, J. W., Richey, L. R., Gardner, J. S., Cha, J. N., & Bartl, M. H. (2008). Discovery of a diamond-based photonic crystal structure in beetle scales. *Physical Review E*, *77*(5). doi:10.1103/physreve.77.050904

Ghiradella, H. (1991). Light and color on the wing: structural colors in butterflies and moths. *Applied Optics*, *30*(24), 3492-3500. doi:10.1364/ao.30.003492

Ghoshal, A., Eck, E., & Morse, D. E. (2016a). Biological analogs of RGB pixelation yield white coloration in giant clams. *Optica*, *3*(1), 108-11. doi:10.1364/optica.3.000108

Ghoshal, A., Eck, E., Gordon, M., & Morse, D. E. (2016b). Wavelength-specific forward scattering of light by Bragg-reflective iridocytes in giant clams. *Journal of The Royal Society Interface*, *13*(120), 20160285. doi:10.1098/rsif.2016.0285

Giraldo, M. A., Yoshioka, S., Liu, C., & Stavenga, D. G. (2016). Coloration mechanisms and phylogeny of *Morpho* butterflies. *Journal of Experimental Biology*, *219*(24), 3936-44. doi:10.1242/jeb.148726

Glover, B. J., & Whitney, H. M. (2010). Structural colour and iridescence in plants: the poorly studied relations of pigment colour. *Annals of botany*, *105*(4), 505-11. doi:10.1093/aob/mcq007

Gordon, R., Losic, D., Tiffany, M. A., Nagy, S. S., & Sterrenburg, F. A. S. (2009). The Glass Menagerie: diatoms for novel applications in nanotechnology. *Trends in Biotechnology*, *27*(2), 116-27. doi:10.1016/j.tibtech.2008.11.003

Gould, K. S., & Lee, D. W. (1996). Physical and Ultrastructural Basis of Blue Leaf Iridescence in Four Malaysian Understory Plants. *American Journal of Botany*, *83*(1), 45-50. doi:10.2307/2445952

Graham, R. M., Lee, D. W., & Norstog, K. (1993). Physical and Ultrastructural Basis of Blue Leaf Iridescence in Two Neotropical Ferns. *American Journal of Botany*, *80*(2), 198-203. doi:10.2307/2445040

Gur, D., Leshem, B., Pierantoni, M., Farstey, V., Oron, D., Weiner, S., & Addadi, L. (2015). Structural Basis for the Brilliant Colors of the Sapphirinid Copepods. *Journal of the American Chemical Society*, *137*(26), 8408-11. doi:10.1021/jacs.5b05289

Hecht, E. (2017). *Optics (5th edition)*. Essex: Pearson.

Hunt, T., Bergsten, J., Levkanicova, Z., Papadopoulou, A., Saint John, O., Wild, R., et al. (2007). A Comprehensive Phylogeny of Beetles Reveals the Evolutionary Origins of a Superradiation. *Science*, *318*(5858), 1913-6. doi:10.1126/science.1146954

Hwang, J., Song, M. H., Park, B., Nishimura, S., Toyooka, T., Wu, J. W., et al. (2005). Electro-tunable optical diode based on photonic bandgap liquid-crystal heterojunctions. *Nature Materials*, *4*(5), 383-7. doi:10.1038/nmat1377

Hébant, C., & Lee, D. W. (1984). Ultrastructural Basis and Developmental Control of Blue Iridescence in Selaginella Leaves. *American Journal of Botany*, *71*(2), 216-9. doi:10.2307/2443748

Ingram, A. L., & Parker, A. R. (2008). A review of the diversity and evolution of photonic structures in butterflies, incorporating the work of John Huxley (The Natural History Museum, London from 1961 to 1990). *Philosophical Transactions of the Royal Society B: Biological Sciences*, *363*(1502), 2465-80. doi:10.1098/rstb.2007.2258

Jacobs, M., Lopez-Garcia, M., Phrathep, O. P., Lawson, T., Oulton, R., & Whitney, H. M. (2016). Photonic multilayer structure of *Begonia* chloroplasts enhances photosynthetic efficiency. *Nature Plants*, *2*(11), 16162. doi:10.1038/nplants.2016.162

Jewell, S. A., Vukusic, P., & Roberts, N. W. (2007). Circularly polarized colour reflection from helicoidal structures in the beetle *Plusiotis boucardi*. *New Journal of Physics*, *9*(4), 99. doi:10.1088/1367-2630/9/4/099

Jiang, T., Peng, Z., Wu, W., Shi, T., & Liao, G. (2014). Gas sensing using hierarchical micro/nanostructures of *Morpho* butterfly scales. *Sensors and Actuators, A: Physical*, *213*, 63-69. doi:10.1016/j.sna.2014.04.002

Joannopoulos, J. D., Johnson, S. G., Winn, J. N., & Meade, R. D. (2008). *Photonic Crystals: Molding the Flow of Light*. Princeton University Press.

Johansen, V. E. (2014). Optical role of randomness for structured surfaces. *Applied Optics*, *53*(11), 2405-15. doi:10.1364/ao.53.002405

Johansen, V. E., Thamdrup, L. H., Smistrup, K., Nielsen, T., Sigmund, O., & Vukusic, P. (2015). Designing visual appearance using a structured surface. *Optica*, *2*(3), 239-45. doi:10.1364/optica.2.000239

Johnson, S., & Joannopoulos, J. (2001). Block-iterative frequency-domain methods for Maxwell's equations in a planewave basis. *Optics Express*, *8*(3), 173-90. doi:10.1364/oe.8.000173

Jordan, T. M., Partridge, J. C., & Roberts, N. W. (2012). Non-polarizing broadband multilayer reflectors in fish. *Nature Photonics*, *6*(11), 759-63. doi:10.1038/nphoton.2012.260

Jordan, T. M., Wilby, D., Chiou, T.-H., Feller, K. D., Caldwell, R. L., Cronin, T. W., & Roberts, N. W. (2016). A shape-anisotropic reflective polarizer in a stomatopod crustacean. *Scientific Reports*, *6*, 21744. doi:10.1038/srep21744

Kientz, B., Luke, S., Vukusic, P., Péteri, R., Beaudry, C., Renault, T., et al. (2016). A unique self-organization of bacterial sub-communities creates iridescence in *Cellulophaga lytica* colony biofilms. *Scientific Reports*, *6*, 19906. doi:10.1038/srep19906

Kieu, K., Li, C., Fang, Y., Cohoon, G., Herrera, O. D., Hildebrand, M., et al. (2014). Structure-based optical filtering by the silica microshell of the centric marine diatom *Coscinodiscus wailesii*. *Optics Express*, *22*(13), 15992-9. doi:10.1364/oe.22.015992

Kinoshita, S. (2008). *Structural Colors in the Realm of Nature*. Singapore: World Scientific Publishing. doi:10.1142/9789812709752

Kinoshita, S., & Yoshioka, S. (2005). Structural Colors in Nature: The Role of Regularity and Irregularity in the Structure. *ChemPhysChem*, *6*(8), 1442-59. doi:10.1002/cphc.200500007

Kinoshita, S., Yoshioka, S., & Miyazaki, J. (2008). Physics of structural colors. *Reports on Progress in Physics*, *71*(7), 076401. doi:10.1088/0034-4885/71/7/076401

Kinoshita, S., Yoshioka, S., Fujii, Y., & Okamoto, N. (2002). Photophysics of structural color in the Morpho butterflies. *Forma*, *17*(2), 103-21.

Land, M. F. (1972). The physics and biology of animal reflectors. *Progress in Biophysics and Molecular Biology*, *24*, 75-106. doi:10.1016/0079-6107(72)90004-1

Lathi, B. P. (1998). *Signal Processing and Linear Systems*. Oxford: Oxford University Press.

Lee, D. W. (1991). Ultrastructural basis and function of iridescent blue colour of fruits in *Elaeocarpus*. *Nature*, *349*(6306), 260-2. doi:10.1038/349260a0

Lee, R. T., & Smith, G. S. (2009). Detailed electromagnetic simulation for the structural color of butterfly wings. *Applied Optics*, *48*(21), 4177-90. doi:10.1364/ao.48.004177

Li, L., Kolle, S., Weaver, J. C., Ortiz, C., Aizenberg, J., & Kolle, M. (2015). A highly conspicuous mineralized composite photonic architecture in the translucent shell of the blue-rayed limpet. *Nature Communications*, *6*, 6322. doi:10.1038/ncomms7322

Liu, F., Yin, H., Dong, B., Qing, Y., Zhao, L., Meyer, S., & Liu, X. (2008). Inconspicuous structural coloration in the elytra of beetles *Chlorophila obscuripennis* (Coleoptera). *Physical Review E, 77(1), 012901*. doi: 10.1103/PhysRevE.77.012901

Lowry, J. B., & Lee, D. W. (1975). Physical basis and ecological significance of iridescence in blue plants. *Nature*, *254*(5495), 50-1. doi:10.1038/254050a0

Luke, S. M., Hallam, B. T., & Vukusic, P. (2010). Structural optimization for broadband scattering in several ultra-thin white beetle scales. *Applied Optics*, *49*(22), 4246-54. doi:10.1364/ao.49.004246

Mason, C. W. (1923). Structural Colors in Feathers. I. *The Journal of Physical Chemistry*, *27*(3), 201-51. doi:10.1021/j150228a001

Michelson, A. A. (1911). LXI. On metallic colouring in birds and insects. *Philosophical Magazine Series 6*, *21*(124), 554-67. doi:10.1080/14786440408637061

Michielsen, K., & Stavenga, D. G. (2008). Gyroid cuticular structures in butterfly wing scales: biological photonic crystals. *Journal of The Royal Society Interface*, *5*(18), 85-94. doi:10.1098/rsif.2007.1065

Michielsen, K., De Raedt, H., & Stavenga, D. G. (2010). Reflectivity of the gyroid biophotonic crystals in the ventral wing scales of the Green Hairstreak butterfly, *Callophrys rubi*. *Journal of The Royal Society Interface*, *7*(46), 765-71. doi:10.1098/rsif.2009.0352

Middleton, R., Steiner, U., & Vignolini, S. (2017). Chapter 17. Bio-mimetic Structural Colour using Biopolymers. *Bio-inspired Polymers*. The Royal Society of Chemistry. doi:10.1039/9781782626664-00555

Mouchet, S. R., Van Hooijdonk, E., Welch, V. L., Louette, P., Colomer, J.-F., Su, B.-L., & Deparis, O. (2016). Liquid-induced colour change in a beetle: the concept of a photonic cell. *Scientific Reports*, *6*, 19322. doi:10.1038/srep19322

Mäthger, L. M., Denton, E. J., Marshall, N. J. & Hanlon, R.T. (2009). Mechanisms and behavioural functions of structural coloration in cephalopods. *Journal of The Royal Society Interface*, *6*(Suppl 2), S149-63. doi:10.1098/rsif.2008.0366.focus

Nakamura, E., Yoshioka, S., & Kinoshita, S. (2008). Structural Color of Rock Dove's Neck Feather. *Journal of the Physical Society of Japan*, *77*(12), 124801. doi:10.1143/jpsj.77.124801

Neville, A. C., & Caveney, S. (1969). Scarabaeid beetle exocuticle as an optical analogue of cholesteric liquid crystals. *Biological reviews*, *44*(4), 531-62. doi:10.1111/j.1469-185x.1969.tb00611.x

Nijhout, H. F. (1985). The Developmental Physiology of Color Patterns in Lepidoptera. *Advances in Insect Physiology 18*,181-247 doi:10.1016/s0065-2806(08)60041-7

Noh, H., Liew, S. F., Saranathan, V., Mochrie, S. G. J., Prum, R. O., Dufresne, E. R., & Cao, H. (2010). How Noniridescent Colors Are Generated by Quasi-ordered Structures of Bird Feathers. *Advanced Materials*, *22*(26-27), 2871-80. doi:10.1002/adma.200903699

Noyes, J. A., Vukusic, P., & Hooper, I. R. (2007). Experimental method for reliably establishing the refractive index of buprestid beetle exocuticle. *Optics Express*, *15*(7), 4351-8. doi:10.1364/oe.15.004351

Noyes, J., Sumper, M., & Vukusic, P. (2008). Light manipulation in a marine diatom. *Journal of Materials Research*, *23*(12), 3229-35. doi:10.1557/jmr.2008.0381

Onelli, O. D., van de Kamp, T., Skepper, J. N., Powell, J., Santos Rolo, dos, T., Baumbach, T., & Vignolini, S. (2017). Development of structural colour in leaf beetles. *Scientific Reports*, *7*, 1373. doi:10.1038/s41598-017-01496-8

Oskooi, A. F., Roundy, D., Ibanescu, M., Bermel, P., Joannopoulos, J. D., & Johnson, S. G. (2010). Meep: A flexible free-software package for electromagnetic simulations by the FDTD method. *Computer Physics Communications*, *181*(3), 687-702. doi:10.1016/j.cpc.2009.11.008

Parker, A. R. (1998). The diversity and implications of animal structural colours. *Journal of Experimental Biology*, *201*(16), 2343-7.

Parker, A. R. (2000). 515 million years of structural colour. *Journal of Optics A: Pure and Applied Optics*, *2*(6), R15-28. doi:10.1088/1464-4258/2/6/201

Parker, A. R. (2005). A geological history of reflecting optics. *Journal of The Royal Society Interface*, *2*(2), 1-17. doi:10.1098/rsif.2004.0026

Parker, A. R., McPhedran, R. C., McKenzie, D. R., & Botten, L. C. (2001). Photonic engineering. Aphrodite's iridescence. *Nature*, (409), 36-37.

Prum, R. O., & Torres, R. H. (2003a). A Fourier Tool for the Analysis of Coherent Light Scattering by Bio-Optical Nanostructures. *Integrative and Comparative Biology*, *43*(4), 591-602. doi:10.1093/icb/43.4.591

Prum, R. O., & Torres, R. H. (2003b). Structural colouration of avian skin: convergent evolution of coherently scattering dermal collagen arrays. *Journal of Experimental Biology*, *206*(14), 2409-29. doi:10.1242/jeb.00431

Prum, R. O. (2006). Anatomy, physics, and evolution of structural colors. In G. E. Hill & K. J. McGraw (Eds.), *Bird coloration* (Vol. 1, pp. 295–353). Cambridge, MA: Harvard University Press.

Prum, R. O., & Torres, R. H. (2013). Fourier Blues: Structural Coloration of Biological Tissues. In *Excursions in Harmonic Analysis, Volume 2, Applied and Numerical Harmonic Analysis*. New York: Springer. doi:10.1007/978-0-8176-8379-5_20

Prum, R. O., Morrison, R. L., & Eyck, Ten, G. R. (1994). Structural color production by constructive reflection from ordered collagen arrays in a bird (*Philepitta castanea: Eurylaimidae*). *Journal of Morphology*, *222*(1), 61-72. doi:10.1002/jmor.1052220107

Prum, R. O., Torres, R. H., Williamson, S., & Dyck, J. (1998). Coherent light scattering by blue feather barbs. *Nature*, *396*(6706), 28-39. doi:10.1038/23838

Prum, R. O., Torres, R., Williamson, S., & Dyck, J. (1999). Two-dimensional Fourier analysis of the spongy medullary keratin of structurally coloured feather barbs. *Proceedings of the Royal Society B: Biological Sciences*, *266*(1414), 13-22. doi:10.1098/rspb.1999.0598

Rayleigh, L. (1919). VII. On the optical character of some brilliant animal colours. *Philosophical Magazine Series 6*, *37*(217), 98-111. doi:10.1080/14786440108635867

Saba, M., Wilts, B. D., Hielscher, J., & Schröder-Turk, G. E. (2014). Absence of Circular Polarisation in Reflections of Butterfly Wing Scales with Chiral Gyroid Structure. *Materials Today: Proceedings*, *1*, 193-208. doi:10.1016/j.matpr.2014.09.023

Saito, A., Miyamura, Y., Nakajima, M., Ishikawa, Y., Sogo, K., Kuwahara, Y., & Hirai, Y. (2006). Reproduction of the Morpho blue by nanocasting lithography. *Journal of Vacuum Science & Technology B: Microelectronics and Nanometer Structures Processing, Measurement, and Phenomena, 24*(6), 3248-51. doi:10.1116/1.2395950

Saito, A., Shibuya, T., Yonezawa, M., Akai-Kasaya, M., & Kuwahara, Y. (2013). Simulation analysis on the optical role of the number of randomly arranged nano-trees on theMorphobutterfly's scale. In *Proceedings Volume 8686, Bioinspiration, Biomimetics, and Bioreplication,* 86860J. doi:10.1117/12.2012036

Saito, A., Yonezawa, M., Murase, J., Juodkazis, S., Mizeikis, V., Akai-Kasaya, M., & Kuwahara, Y. (2011). Numerical Analysis on the Optical Role of Nano-Randomness on the *Morpho* Butterfly's Scale. *Journal of Nanoscience and Nanotechnology*, *11*(4), 2785-92. doi:10.1166/jnn.2011.3906

Saito, A., Yoshioka, S.-Y., & Kinoshita, S. (2004). Reproduction of the *Morpho* butterfly's blue: arbitration of contradicting factors. In *Proceedings Volume 5526, Optical Systems Degradation, Contamination, and Stray Light: Effects, Measurements, and Control*, 188-94. doi:10.1117/12.559086

Schoen, A. H. (1970). *Three dimensional Euclidean space partitioned into interpenetrating labyrinths by infinite periodic minimal surfaces without self intersections*, NASA-TN-D-5541, C-98. United States: NASA.

Schröder-Turk, G. E., Wickham, S., Averdunk, H., Brink, F., Gerald, J. D. F., Poladian, L., & Hyde, S. T. (2011). The chiral structure of porous chitin within the wing-scales of *Callophrys rubi. Journal of Structural Biology*, *174*(2), 290-5. doi:10.1016/j.jsb.2011.01.004

Schultz, T. D., & Bernard, G. D. (1989). Pointillistic mixing of interference colours in cryptic tiger beetles. *Nature*, *337*(6202), 72-3. doi:10.1038/337072a0

Seago, A. E., Brady, P., Vigneron, J. P., & Schultz, T. D. (2009). Gold bugs and beyond: a review of iridescence and structural colour mechanisms in beetles (Coleoptera). *Journal of The Royal Society Interface*, *6*(Suppl 2), S165-84. doi:10.1098/rsif.2008.0354.focus

Sellers, S. R., Man, W., Saba, M., & Florescu, M. (2017). Local self-uniformity in photonic networks. *Nature Communications*, *8*, 14439. doi: 10.1038/ncomms14439

Sharma, V., Crne, M., Park, J. O., & Srinivasarao, M. (2009). Structural origin of circularly polarized iridescence in jeweled beetles. *Science*, *325*(5939), 449-51. doi: 10.1126/science.1172051

Shawkey, M. D., Saranathan, V., Palsdottir, H., Crum, J., Ellisman, M. H., Auer, M., & Prum, R. O. (2009). Electron tomography, three-dimensional Fourier analysis and colour prediction of a three-dimensional amorphous biophotonic nanostructure. *Journal of The Royal Society Interface*, *6*(Suppl 2), S213-20. doi:10.1098/rsif.2008.0374.focus

Song, B., Johansen, V. E., Sigmund, O., & Shin, J. H. (2017). Reproducing the hierarchy of disorder for Morpho-inspired, broad-angle color reflection. *Scientific Reports*, *7*, 46023. doi:10.1038/srep46023

Starkey, T., & Vukusic, P. (2013). Light manipulation principles in biological photonic systems. *Nanophotonics*, *2*(4), 289-307. doi:10.1515/nanoph-2013-0015

Stavenga, D. G., Leertouwer, H. L., Marshall, N. J., & Osorio, D. (2011a). Dramatic colour changes in a bird of paradise caused by uniquely structured breast feather barbules. *Proceedings of the Royal Society B: Biological Sciences*, *278*(1715), 2098-2104. doi:10.1098/rspb.2010.2293

Stavenga, D. G., Wilts, B. D., Leertouwer, H. L., & Hariyama, T. (2011b). Polarized iridescence of the multilayered elytra of the Japanese jewel beetle, *Chrysochroa fulgidissima*. *Philosophical Transactions of the Royal Society B: Biological Sciences*, *366*(1565), 709-723. doi:10.1098/rstb.2010.0197

Steinbrecht, R. A., Mohren, W., & Schneider, D. (1985). Cuticular interference reflectors in the golden pupae of danaine butterflies. *Proceedings of the Royal Society of London B: Biological Sciences*, *226*(1244), 367-390. doi: 10.1098/rspb.1985.0100

Strout, G., Russell, S. D., Pulsifer, D. P., Erten, S., Lakhtakia, A., & Lee, D. W. (2013). Silica nanoparticles aid in structural leaf coloration in the Malaysian tropical rainforest understorey herb *Mapania caudata*. *Annals of botany*, *112*(6), 1141-8. doi:10.1093/aob/mct172

Sumper, M., & Brunner, E. (2006). Learning from Diatoms: Nature's Tools for the Production of Nanostructured Silica. *Advanced Functional Materials*, *16*(1), 17-26. doi:10.1002/adfm.200500616

Sun, J., Bhushan, B., & Tong, J. (2013). Structural coloration in nature. *RSC Advances*, *3*(35), 14862-89. doi:10.1039/c3ra41096j

Thomas, K. R., Kolle, M., Whitney, H. M., Glover, B. J., & Steiner, U. (2010). Function of blue iridescence in tropical understorey plants. *Journal of The Royal Society Interface*, *7*(53), 1699-1707. doi:10.1098/rsif.2010.0201

Toninelli, C. (2007). *Light transport in photonic structures: interplay between order and disorder* (pp. 17–26). PhD thesis, LENS, Florence.

Trzeciak, T. M., & Vukusic, P. (2009). Photonic crystal fiber in the polychaete worm *Pherusa* sp. *Physical Review E*, *80*(6), 061908.

Vignolini, S., Gregory, T., Kolle, M., Lethbridge, A., Moyroud, E., Steiner, U., et al. (2016). Structural colour from helicoidal cell-wall architecture in fruits of *Margaritaria nobilis*. *Journal of The Royal Society Interface, 13*(124), 20160645. doi: 10.1098/rsif.2016.0645

Vignolini, S., Moyroud, E., Glover, B. J., & Steiner, U. (2013). Analysing photonic structures in plants. *Journal of The Royal Society Interface*, *10*(87), 20130394. doi:10.1098/rsif.2013.0394

Vignolini, S., Moyroud, E., Hingant, T., Banks, H., Rudall, P. J., Steiner. U., & Glover, B. (2015a). Is floral iridescence a biologically relevant cue in plant-pollinator signalling? A response to van der Kooi et al.(2014b). *New Phytologist 205*(1), 21-22. doi: 10.1111/nph.13178

Vignolini, S., Moyroud, E., Hingant, T., Banks, H., Rudall, P. J., Steiner, U., & Glover, B. J. (2015b). The flower of *Hibiscus trionum* is both visibly and measurably iridescent. *New Phytologist*, *205*(1), 97-101. doi:10.1111/nph.12958

Vignolini, S., Rudall, P. J., Rowland, A. V., Reed, A., Moyroud, E., Faden, R. B., et al. (2012). Pointillist structural color in Pollia fruit. *Proceedings of the National Academy of Sciences*, *109*(39), 15712-5. doi:10.1073/pnas.1210105109

Vukusic, P., & Sambles, J. R. (2003). Photonic structures in biology. *Nature*, *424*(6950), 852-5. doi:10.1038/nature01941

Vukusic, P., & Stavenga, D. G. (2009). Physical methods for investigating structural colours in biological systems. *Journal of The Royal Society Interface*, *6*(Suppl_2), S133-48. doi:10.1098/rsif.2008.0386.focus

Vukusic, P., Hallam, B., & Noyes, J. (2007). Brilliant Whiteness in Ultrathin Beetle Scales. *Science*, *315*(5810), 348. doi:10.1126/science.1134666

Vukusic, P., Sambles, J. R., & Lawrence, C. R. (2000). Structural colour: Colour mixing in wing scales of a butterfly. *Nature*, *404*(6777), 457. doi:10.1038/35006561

Vukusic, P., Sambles, J. R., Lawrence, C. R., & Wootton, R. J. (1999). Quantified interference and diffraction in single Morpho butterfly scales. *Proceedings of the Royal Society. Series B: Biological Sciences*, *266*(1427), 1403-11. doi:10.1098/rspb.1999.0794

Whitney, H. M., Kolle, M., Andrew, P., Chittka, L., Steiner, U., & Glover, B. J. (2009). Floral Iridescence, Produced by Diffractive Optics, Acts As a Cue for Animal Pollinators. *Science*, *323*(5910), 130-3. doi:10.1126/science.1166256

Wickham, S., Large, M. C. J., Poladian, L., & Jermiin, L. S. (2006). Exaggeration and suppression of iridescence: the evolution of two-dimensional butterfly structural colours. *Journal of The Royal Society Interface*, *3*(6), 99-109. doi:10.1098/rsif.2005.0071

Wiersma, D. S. (2013). Disordered photonics. *Nature Photonics*, *7*(3), 188-96. doi:10.1038/nphoton.2013.29

Wikimedia Commons, Kuribo (2008). *Satyr Tragopan, captive, Osaka*. Satyr Tragopan Osaka.jpg, licensed under CC BY-SA 3.0.

Wikimedia Commons, William H. Majoros (2010). *Eastern Bluebird*. 7Z1E5531.jpg, licensed under CC BY-SA 3.0.

Wilts, B. D., Michielsen, K., De Raedt, H., & Stavenga, D. G. (2012a). Iridescence and spectral filtering of the gyroid-type photonic crystals in *Parides sesostris* wing scales. *Interface Focus*, *2*(5), 681-7. doi:10.1098/rsfs.2011.0082

Wilts, B. D., Michielsen, K., De Raedt, H., & Stavenga, D. G. (2014a). Sparkling feather reflections of a bird-of-paradise explained by finite-difference time-domain modeling. *Proceedings of the National Academy of Sciences*, *111*(12), 4363-8. doi:10.1073/pnas.1323611111

Wilts, B. D., Michielsen, K., Kuipers, J., De Raedt, H., & Stavenga, D. G. (2012b). Brilliant camouflage: photonic crystals in the diamond weevil, *Entimus imperialis*. *Proceedings of the Royal Society B: Biological Sciences*, *279*(1738), 2524-30. doi:10.1098/rspb.2011.2651

Wilts, B. D., Sheng, X., Holler, M., Diaz, A., Guizar-Sicairos, M., Raabe, J., et al. (2017a). Evolutionary-Optimized Photonic Network Structure in White Beetle Wing Scales. *Advanced Materials*, 1702057. doi:10.1002/adma.201702057

Wilts, B. D., Whitney, H. M., Glover, B. J., Steiner, U., & Vignolini, S. (2014b). Natural Helicoidal Structures: Morphology, Self-assembly and Optical Properties. *Materials Today: Proceedings*, *1*, 177-85. doi:10.1016/j.matpr.2014.09.021

Wilts, B. D., Zubiri, B. A., Klatt, M. A., Butz, B., Fischer, M. G., Kelly, S. T., et al. (2017b). Butterfly gyroid nanostructures as a time-frozen glimpse of intracellular membrane development. *Science Advances*, *3*(4), e1603119. doi:10.1126/sciadv.1603119

Wolf, E. (2007). *Introduction to the Theory of Coherence and Polarization of Light*. Cambridge: Cambridge University Press.

Yablonovitch, E. (1993). Photonic band-gap structures. *Journal of the Optical Society of America B, 10*(2), 283-295. doi: 10.1364/JOSAB.10.000283

Yong, J., Chen, F., Yang, Q., Du, G., Shan, C., Bian, H., et al. (2015). Bioinspired transparent underwater superoleophobic and anti-oil surfaces. *Journal of Materials Chemeistry A*, *3*(18), 9379-84. doi:10.1039/c5ta01104c

Yoshioka, S., & Kinoshita, S. (2007). Polarization-sensitive color mixing in the wing of the Madagascan sunset moth. *Optics Express*, *15*(5), 2691-2701. doi:10.1364/oe.15.002691

Yoshioka, S., & Kinoshita, S. (2009). Optical effects of highly curved multilayer structure found in the scale of structurally colored moth. In *Proceedings Volume 7401, Biomimetics and Bioinspiration*, 740105. doi:10.1117/12.824861

Yun, W.-B., Kirz, J., & Sayre, D. (1987). Observation of the soft X-ray diffraction pattern of a single diatom. *Acta Crystallographica Section A: Foundations of Crystallography*, *43*(1), 131-3. doi:10.1107/s0108767387099744

Zi, J., Yu, X., Li, Y., Hu, X., Xu, C., Wang, X., et al. (2003). Coloration strategies in peacock feathers. *Proceedings of the National Academy of Sciences*, *100*(22), 12576-8. doi:10.1073/pnas.2133313100

van der Kooi, C. J., Dyer, A. G., & Stavenga, D. G. (2015). Is floral iridescence a biologically relevant cue in plant-pollinator signaling? *New Phytologist*, *205*(1), 18-20. doi:10.1111/nph.13066

van der Kooi, C. J., Wilts, B. D., Leertouwer, H. L., Staal, M., Elzenga, J. T. M., & Stavenga, D. G. (2014). Iridescent flowers? Contribution of surface structures to optical signaling. *New Phytologist*, *203*(2), 667-73. doi:10.1111/nph.12808

Åkerlind, C., Arwin, H., Hallberg, T., Landin, J., Gustafsson, J., Kariis, H., & Järrendahl, K. (2015). Scattering and polarization properties of the scarab beetle *Cyphochilus insulanus* cuticle. *Applied Optics*, *54*(19), 6037-45. doi:10.1364/ao.54.006037